Biophysical Journal
Article

Biophysical Society

Criticality and Adaptivity in Enzymatic Networks

Paul J. Steiner,[1] Ruth J. Williams,[1,2,*] Jeff Hasty,[1,3,4,5,*] and Lev S. Tsimring[1,5,*]
[1]BioCircuits Institute, [2]Department of Mathematics, [3]Molecular Biology Section, Division of Biological Sciences, [4]Department of Bioengineering, and [5]San Diego Center for Systems Biology, University of California, San Diego, La Jolla, California

ABSTRACT The contrast between the stochasticity of biochemical networks and the regularity of cellular behavior suggests that biological networks generate robust behavior from noisy constituents. Identifying the mechanisms that confer this ability on biological networks is essential to understanding cells. Here we show that queueing for a limited shared resource in broad classes of enzymatic networks in certain conditions leads to a critical state characterized by strong and long-ranged correlations between molecular species. An enzymatic network reaches this critical state when the input flux of its substrate is balanced by the maximum processing capacity of the network. We then consider enzymatic networks with adaptation, when the limiting resource (enzyme or cofactor) is produced in proportion to the demand for it. We show that the critical state becomes an attractor for these networks, which points toward the onset of self-organized criticality. We suggest that the adaptive queueing motif that leads to significant correlations between multiple species may be widespread in biological systems.

INTRODUCTION

Transcription, translation, and signaling are stochastic processes often dominated by small-number effects. Yet overall, cellular behaviors proceed with remarkable predictability and regularity. How are such robust and reliable systems built from noisy elements? Previous work has suggested that some networks actively suppress noise and others harness it (1–3), with particular attention paid to noise in the concentrations of protein species. Certain regulatory networks achieve high sensitivity by exploiting mechanisms such as substrate competition and molecular titration in which only relative levels of molecular species matter (4,5). Then, correlations between different proteins are important and the noise in the level of a single species is less relevant. Here we show that competition for limited shared resources in a broad class of enzymatic networks can lead to such strong correlations and furthermore, that network adaptation can make such highly correlated states robust to changes in parameters. The state of an enzymatic network characterized by strong and long-ranged correlations can naturally be interpreted as a critical state, and the adaptation leading toward this regime can likewise be interpreted as a mechanism for self-organized criticality. In a recent work, Ray et al. (6) demonstrated that expression of a single enzyme may have a profound effect on the physiology of the whole cell by driving the metabolic network across a threshold above which cells undergo growth arrest due to the toxicity of overabundant metabolite. They showed that cells may optimize biomass production by balancing the cell growth and toxicity caused by the metabolite overproduction that occurs in the vicinity of the critical state of the metabolic network.

Critical phenomena associated with phase transitions have received much attention as possible explanations for the complexity observed in nature, because critical systems exhibit large fluctuations, slow dynamics, and strong correlations. In particular, self-organized critical systems—those that naturally tend to their critical states—have been suggested to explain phenomena as diverse as earthquakes (7) and evolution (8). Recent work has indicated a possibility of near-criticality in single-enzyme systems (9) and suggested that multicellular organisms harness criticality in development (10).

Traditionally, enzymatic networks have been modeled deterministically using the Michaelis-Menten formalism (11). More recently, the statistical properties of enzymatic pathways have begun to attract significant attention (12–16). Levine and Hwa (12) theoretically studied stochastic fluctuations in different classes of metabolic pathways and found that steady-state fluctuations of intermediaries are effectively uncorrelated. This result, however, is linked to the important assumption that different enzymatic steps are catalyzed by different enzymes. While many enzymes are

Submitted March 15, 2016, and accepted for publication July 28, 2016.
*Correspondence: williams@math.ucsd.edu or hasty@ucsd.edu or ltsimring@ucsd.edu
Editor: Richard Bertram.
http://dx.doi.org/10.1016/j.bpj.2016.07.036

highly substrate-specific, many also target multiple substrates. For example, RNA transcripts must compete for translation by a limited number of ribosomes (17,18). Bacterial sigma factors are coupled by their competition for RNA polymerases (19). In yeast, ultrasensitivity of Wee1 inactivation is believed to be generated by competition between Wee1 and other Cdk1 substrates for phosphorylation by Cdk1 (4). In mice, two F-box protein paralogs FBXL3 and FBXL21 (as part of an SCF complex) compete for binding of CRY proteins that act as circadian clock inhibitors (20). Degradation of many different proteins within the same cell is often enabled by a small group of enzymes such as the ClpXP protease in bacteria or the 26S proteasome in eukaryotes.

Previous work has shown that proteins degraded by a common protease exhibit strong correlations near the balance point where the total synthesis rate of the proteins matches the processing capacity of the protease (13,14). This coupling mechanism has been recently used to tightly synchronize two independent genetic oscillators (21). It has been shown (22,23) that posttranslation regulation via microRNA also leads to strong correlations among competing endogenous RNAs.

Here we consider a broad class of enzymatic networks in which different protein species either are interconverted by a common enzyme or share a common cofactor. These enzymatic networks with limited shared resources model a variety of phenomena in complex biological systems, including enzyme promiscuity in metabolic networks (24) and multisite phosphorylation of a protein (25). We use the mathematical theory of multiclass queues (26–28) to describe the statistical properties of protein fluctuations in steady state and demonstrate that in certain parameter regimes these networks exhibit critical behavior characterized by strong and long-ranged correlations between molecular species.

For a system with fixed limited resources, the critical state emerges only when the system is tuned to be near the balance point. However, allowing enzyme or cofactor levels to adapt to the size of the protein queue makes critical behavior robust to changes in system parameters. This type of adaptivity has been found in a number of similar enzymatic contexts, such as bacterial chemotaxis (29), signal transduction in the retina (30), calcium homeostasis (31), yeast osmoregulation (32), and temperature compensation in circadian clocks (33). Furthermore, in several recent works, adaptivity of general enzymatic networks was considered analytically and numerically in deterministic approximations (30,34). We find that augmenting our enzymatic networks with adaptive feedback regulation gives rise to critical behavior in a broad region of parameter space, eliminating the need to tune a system to its balance point and indicating that these systems may exhibit self-organized criticality. Together, our results suggest that adaptive queueing may be a general principle that plays a pivotal role in conferring robustness on native biological circuits and a designer's tool for constructing synthetic networks.

MATERIALS AND METHODS

Shared resource-limited enzymatic networks

We study four classes of enzymatic networks in which reactions are rate-limited by a common resource (Fig. 1, *A–D*). Specifically, we consider competition for a fixed number of enzyme molecules that perform all enzymatic reactions (Fig. 1, *A* and *B*), or competition for a consumable cofactor produced at a fixed rate that is required for all enzymatic reactions (Fig. 1, *C* and *D*). For the parallel network with a shared enzyme (Fig. 1 *A*), we assume that L copies of the enzyme E catalyze degradation of n proteins $X_1, \ldots, X_n$. However, the same model can be applied to conversion of substrates X_i into their corresponding products X_i^*. The biochemical reactions in this system are:

$$\begin{aligned} &\varnothing \xrightarrow{\lambda} X_i, \\ &X_i + E \underset{\eta^-}{\overset{\eta^+}{\rightleftharpoons}} X_i E \xrightarrow{\mu} E, \\ &X_i E \xrightarrow{\gamma} E, \\ &X_i \xrightarrow{\gamma} \varnothing. \end{aligned} \tag{1}$$

Here $i = 1, \ldots n$; λ is the synthesis rate of all proteins; $\eta_\pm$ are binding/unbinding rates of proteins to the enzyme; μ is the rate at which an enzyme processes a protein; and γ is the dilution rate of all proteins (bound and unbound).

For the serial network with a shared enzyme (Fig. 1 *B*), we assume that the only input to the system is synthesis of protein X_1 at rate λ, a common pool of L copies of the enzyme E converts X_i into X_{i+1}, and the last stage of enzymatic processing degrades the protein X_n:

$$\begin{aligned} &\varnothing \xrightarrow{\lambda} X_1, \\ &X_i + E \underset{\eta^-}{\overset{\eta^+}{\rightleftharpoons}} X_i E \xrightarrow{\mu} X_{i+1} + E, \quad i = 1, \ldots, n-1, \\ &X_n + E \underset{\eta^-}{\overset{\eta^+}{\rightleftharpoons}} X_n E \xrightarrow{\mu} E, \\ &X_i E \xrightarrow{\gamma} E, \\ &X_i \xrightarrow{\gamma} \varnothing, \quad i = 1, \ldots, n. \end{aligned} \tag{2}$$

Note that a similar system of enzymatic reactions has been studied in a recent work (35) where the authors found a critical slowdown of the cascade response to external perturbations when the system approached maximum capacity.

The last two networks have shared cofactors instead of shared enzymes. For them, we assume that enzymes are not rate-limiting and exclude them from consideration. Instead, we assume that the enzymatic reactions consume a shared cofactor C that is produced at rate λ_C and is degraded at rate γ_C. We consider both a parallel and a serial network. For the parallel network (Fig. 1 *C*), the biochemical reactions are:

$$\begin{aligned} &\varnothing \xrightarrow{\lambda} X_i, \\ &\varnothing \xrightarrow{\lambda_C} C, \\ &X_i + C \underset{\eta^-}{\overset{\eta^+}{\rightleftharpoons}} X_i C \xrightarrow{\mu} \varnothing, \\ &X_i C \xrightarrow{\gamma} \varnothing, \\ &X_i \xrightarrow{\gamma} \varnothing, \\ &C \xrightarrow{\gamma_C} \varnothing, \end{aligned} \tag{3}$$

where $i = 1, \ldots, n$. For the serial network (Fig. 1 *D*), the reactions are:

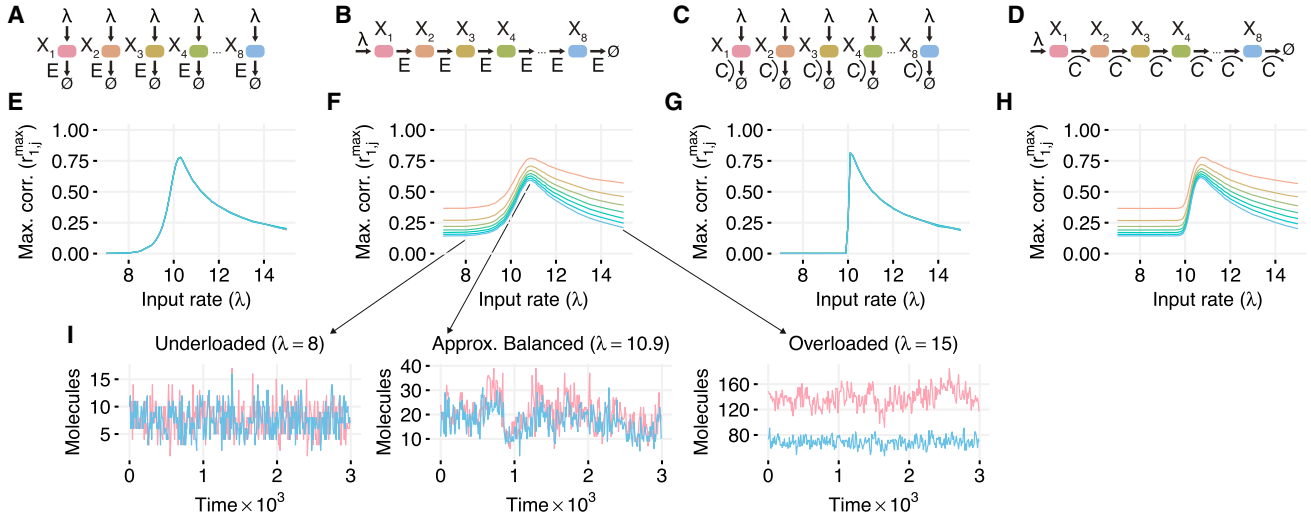

FIGURE 1 Generality of correlation resonance in biochemical networks. For each different type of network (*A–D*), levels of all species are highly correlated at the critical point where the input rate λ is balanced by removal of molecules from the system. (*A*) Parallel network of proteins degraded by a common enzyme. (*B*) Serial network of proteins interconverted by a common enzyme. (*C*) Parallel network of molecules processed by different abundant enzymes that all use a common cofactor. (*D*) Serial network of molecules processed by different abundant enzymes that all use a common cofactor. (*E–H*) Maximum correlations between X_i and X_j (denoted $r_{1j}^{\max}$) for simulations of each network. For the two serial networks, these maximal correlations occur at λ- and j-dependent time delays $\tau_{\max}$. Line color corresponds to the diagrams in (*A–D*). (*I*) Sample trajectories from the underloaded (*left*), approximately balanced (*center*), and overloaded (*right*) regimes of the serial network shown in (*B*). For networks with shared enzymes, the number of enzymes was fixed at $L = 80$. For the networks with a shared cofactor, the cofactor was synthesized at rate $\lambda_C = 80$ and diluted at rate γ. Other parameters were $\gamma = 0.01$, $\mu = 1$, $\eta^+ = 1000$, $\eta^- = 0$, and $L = 80$. To see this figure in color, go online.

$$
\begin{aligned}
&\varnothing \xrightarrow{\lambda} X_1,\\
&\varnothing \xrightarrow{\lambda_C} C,\\
&X_i + C \underset{\eta^-}{\overset{\eta^+}{\rightleftharpoons}} X_i C \xrightarrow{\mu} X_{i+1}, \quad i = 1,\ldots,n-1,\\
&X_n + C \underset{\eta^-}{\overset{\eta^+}{\rightleftharpoons}} X_n C \xrightarrow{\mu} \varnothing,\\
&X_i C \xrightarrow{\gamma} \varnothing,\\
&X_i \xrightarrow{\gamma} \varnothing, \quad i = 1,\ldots,n,\\
&C \xrightarrow{\gamma_C} \varnothing.
\end{aligned}
\tag{4}
$$

We performed numerical simulations of these four systems of biochemical reactions using the direct Gillespie algorithm (36) and computed cross correlations among different substrates in the statistically stationary regime:

$$
r_{ij}(\tau) \equiv \frac{\operatorname{cov}\left[Q_i(t), Q_j(t+\tau)\right]}{\sigma_i \sigma_j}, \tag{5}
$$

where $\operatorname{cov}[Q_i(t), Q_j(t+\tau)] = \langle Q_i(t) Q_j(t+\tau)\rangle - \langle Q_i\rangle\langle Q_j\rangle$ is the covariance between the total number of protein X_i (both free and enzyme-bound) at time t, $Q_i(t)$, and the total number of protein X_j at time $t+\tau$, $Q_j(t+\tau)$, and $\sigma_i = [\langle Q_i^2\rangle - \langle Q_i\rangle^2]^{1/2}$ is the standard deviation of Q_i. For simplicity, we consider the case of irreversible binding where $\eta^- = 0$. Unless noted otherwise, parameters for all simulations described here and below are $n = 8$, $\gamma = \gamma_C = 0.01$, $\mu = 1$, $\eta^+ = 1000$, $\eta^- = 0$, and $L = 80$.

We also obtained analytical results for these systems for the underloaded regime in the zero dilution limit.

Modeling of adaptive enzymatic networks

To investigate the role of adaptation in the dynamics of enzymatic networks with shared resources, we generalize our previous models. Instead of keeping the number of enzymes fixed, we allow molecules of the enzyme to be produced and diluted, with the production rate of the enzymes dependent on the numbers of proteins in the system. We first consider parallel degradation of multiple species (see Fig. 4 *A*). We assume that n proteins $X_1,\ldots,X_n$ are synthesized at rates $\lambda_1,\ldots,\lambda_n$ and degraded by the shared enzyme E that is synthesized at a rate ν that depends on the amount of the proteins present in the system (see below). All species (including E) are diluted at the rate γ. The reactions for the model are:

$$
\begin{aligned}
&\varnothing \xrightarrow{\lambda_i} X_i,\\
&\varnothing \xrightarrow{\nu} E,\\
&X_i + E \underset{\eta^-}{\overset{\eta^+}{\rightleftharpoons}} X_i E \xrightarrow{\mu} E,\\
&X_i E \xrightarrow{\gamma} \varnothing,\\
&X_i \xrightarrow{\gamma} \varnothing,\\
&E \xrightarrow{\gamma} \varnothing,
\end{aligned}
\tag{6}
$$

where the enzyme synthesis rate ν is allowed to take various forms as a function of $Q_i, i = 1,\ldots,n$. Here we consider only the simple case where $\nu(Q_1,\ldots,Q_n) = \alpha\sum_{i=1}^n Q_i$. Similar systems of enzymatic reactions with feedback have been explored in the literature (see, for example, Furusawa and Keneko (34) and He et al. (37)), but only with a single class of substrate for each enzyme.

In the limit of large numbers of all molecules and fast binding-unbinding reactions (the Michaelis-Menten approximation), the system can be described by the mass-action equations for the deterministic variables $\overline{Q}_i$ and $\overline{L}$ that denote ensemble averages of total proteins Q_i and enzyme L, respectively:

$$
\frac{d\overline{Q}_i}{dt} = \lambda_i - \frac{\mu \overline{L}\,\overline{Q}_i}{K_m + \sum_{i=1}^n \overline{Q}_i} - \gamma \overline{Q}_i \quad \text{for} \quad i = 1,\ldots,n, \tag{7}
$$

$$\frac{d\overline{L}}{dt} = \alpha\sum_{i=1}^{n}\overline{Q}_i - \gamma\overline{L}, \tag{8}$$

where $K_m = \eta^-/\eta^+$. The stable stationary solution of Eqs. 7 and 8 in implicit form is:

$$\overline{L} = \frac{\alpha\Lambda}{\gamma}\left[\frac{\mu\overline{L}}{K_m + \gamma\alpha^{-1}\overline{L}} + \gamma\right]^{-1}, \tag{9}$$

$$\overline{Q}_i = \lambda_i\left[\frac{\mu\overline{L}}{K_m + \gamma\alpha^{-1}\overline{L}} + \gamma\right]^{-1}, \tag{10}$$

where $\Lambda = \sum_{i=1}^{n}\lambda_i$. In the strong binding limit $K_m \to 0$, these expressions simplify to explicit formulae:

$$\overline{L} = \frac{\alpha\Lambda}{\mu\alpha + \gamma^2}, \tag{11}$$

$$\overline{Q}_i = \frac{\gamma\lambda_i}{\mu\alpha + \gamma^2}, \quad i = 1, \ldots, n. \tag{12}$$

Interestingly, despite the coupling of all species by enzymatic degradation, the steady-state value of $\overline{Q}_i$ depends only on its own synthesis rate λ_i and not on any other $\lambda_j, j \neq i$. This is a manifestation of the perfect adaptation caused by the integral feedback via the regulated enzyme synthesis (37,38). Similar perfect adaptation is known to play a key role in making bacterial chemotaxis robust against changes in overall concentration of chemoattractants (29). However, an abrupt change in synthesis rate of one of the proteins transiently affects the rate (per molecule) at which proteins are removed from the system, and therefore the abundances of all proteins, as the amount of enzyme evolves to a new balance point (see Fig. 4 *B*).

Substituting $\overline{L}$ from Eq. 11 into $\rho = \Lambda/\overline{L}\mu$, we obtain that, in the stationary state, $\rho = 1 + \gamma^2/(\alpha\mu)$. Thus, for sufficiently large $\alpha \gg \gamma^2/\mu$, the stationary regime is close to balance; however, for smaller α there are not enough copies of the enzyme due to dilution, and the system becomes overloaded. On the other hand, for sufficiently large α, the Michaelis-Menten approximation used in Eq. 7 no longer holds. Indeed, in the strong binding limit the rate of enzymatic degradation is limited by $\mu\min\{Q, L\}$. Therefore, from Eqs. 11 and 12 for $\alpha > \gamma$ and $\overline{Q} < \overline{L}$, there are more copies of the enzyme than arriving proteins, and the system becomes strongly underloaded in the steady state. Therefore, enzymatic adaptation should be effective within the range $\gamma^2/\mu \ll \alpha \ll \gamma$.

We next consider enzymatic adaptation for the serial enzymatic network introduced earlier in Fig. 1 *B*. In addition to the reactions in Eq. 2, we assume that enzymes are synthesized with a rate that is proportional to the total number of proteins in the system Q and are diluted at rate γ_E, with $\gamma = \gamma_E$ for $\gamma \neq 0$ (see Fig. 5 *A*). The reactions in this system are

$$\begin{aligned}
&\varnothing \xrightarrow{\lambda} X_1,\\
&\varnothing \xrightarrow{\nu} E,\\
&X_i + E \underset{\eta^-}{\overset{\eta^+}{\rightleftharpoons}} X_iE \xrightarrow{\mu} X_{i+1} + E \quad i = 1, \ldots, n-1,\\
&X_n + E \underset{\eta^-}{\overset{\eta^+}{\rightleftharpoons}} X_nE \xrightarrow{\mu} E,\\
&X_iE \xrightarrow{\gamma} \varnothing,\\
&X_i \xrightarrow{\gamma} \varnothing, \quad i = 1, \ldots, n,\\
&E \xrightarrow{\gamma} \varnothing.
\end{aligned} \tag{13}$$

The mass-action model of adaptive queueing in a serial network with the continuous variables for ensemble averages $\overline{Q}_i$ and $\overline{L}$ is:

$$\frac{d\overline{Q}_1}{dt} = \lambda - \frac{\mu\overline{L}\,\overline{Q}_1}{K_m + \sum_{j=1}^{n}\overline{Q}_j} - \gamma\overline{Q}_1, \tag{14}$$

$$\frac{d\overline{Q}_i}{dt} = \frac{\mu\overline{L}(\overline{Q}_{i-1} - \overline{Q}_i)}{K_m + \sum_{j=1}^{n}\overline{Q}_j} - \gamma\overline{Q}_i \quad i = 2, \ldots, n, \tag{15}$$

$$\frac{d\overline{L}}{dt} = \alpha\sum_{i=1}^{n}\overline{Q}_i - \gamma\overline{L}. \tag{16}$$

In the strong binding limit $K_m \to 0$, the stationary solution of Eqs. 14–16 is given by

$$\overline{Q}_i = \frac{\lambda\gamma}{\mu\alpha}\frac{1}{(1 + \gamma^2/\mu\alpha)^i}, \tag{17}$$

$$\overline{L} = \frac{\lambda\alpha}{\gamma^2}\left(1 - \frac{1}{(1 + \gamma^2/\mu\alpha)^n}\right). \tag{18}$$

For large $\alpha \gg \gamma^2/\mu$, the number of enzymes in the stationary state approaches the exact balance level $\overline{L}_b = n\lambda/\mu$. A typical transient regime for the eight-stage chain is shown in Fig. 5 *B*. As in the case of adaptive enzymatic degradation in the parallel network, the system adapts to be very near the balance point, but the negative feedback leads to transient ringing in the mean number of proteins and the number of enzymes in the system when parameters are changed.

RESULTS

Criticality in nonadaptive resource-limited enzymatic networks

Fig. 1, *E–H*, depicts the maximum value of the cross correlations $r_{1j}^{\max} = \max_\tau r_{1j}(\tau)$ as a function of λ for the four types of enzymatic networks shown in Fig. 1, *A–D*. All four networks exhibited well-pronounced correlation resonance: when the rate of resource utilization approached the rate of resource availability, all species in the network became highly correlated. This correlation resonance phenomenon is not specific to these examples. We observed similar behavior in networks with reversible binding (Figs. S1 and S2 in the Supporting Material), even when binding constants $\eta^\pm$ are significantly varied (Fig. S3), as well as in more complicated networks with multiple shared cofactors (Fig. S4).

For a detailed analysis, we focus now on the serial shared enzyme network (Fig. 1, *B*, *F*, and *I*). The other three networks behave in a qualitatively similar manner. This system can, for example, represent sequential phosphorylation of a protein by a kinase. When $\rho \equiv n\lambda/(L\mu) \ll 1$, the network is strongly underloaded and the correlation between $Q_1(t)$ and $Q_j(t+\tau)$ is very close to zero for $\tau \leq 0$. However, the system can still exhibit time-delayed correlations that emerge

due to the propagation of fluctuations in X_i downstream via its processing by E and reaches a maximum $r_{1j}^{\max}$ at a small positive delay $\tau_{\max}$ (Fig. 2 *A*, *left*). Interestingly, while correlations at $\tau = 0$ are independent of position in the network, time-shifted correlations decay along the chain (Fig. 2 *A*, *center-left*). Near the balance point, where the input rate λ is equal to the processing capacity $L\mu/n$, even the same-time correlations between all pairs of species are high. This is remarkable, given that X_i can only be introduced at the expense of X_{i-1} (Fig. 2 *A*, *center-right*).

Fig. 2 *B* shows the dependences of $r_{1j}^{\max}$ and $\tau_{\max}$ on the input rate λ. As λ increases, correlations become larger, and become nonzero even for $\tau \leq 0$. In the strongly overloaded regime ($\rho >> 1$), the correlations decay much more slowly than in the underloaded case (Fig. 2 *A*, *right*). The time lag $\tau_{\max}$ at which the cross-correlation coefficients r_{1j} are maximal also becomes much longer. The maximal correlation itself $r_{1j}(\tau_{\max})$ reaches a sharp peak near balance. As λ is increased substantially beyond the balance point, $r_{1j}^{\max}$ decreases, while $\tau_{\max}$ grows linearly (Fig. 2 *B*).

High correlations and slowing of the dynamics are strong indicators of emergent criticality in this enzymatic network. The serial network also allows us to define a distance between two species: the number of enzymatic steps between them. We therefore computed the correlation length L_c for the serial networks that we define as the (linearly interpolated) number of stages at which the maximum cross-correlation coefficient with the first protein is >0.5 (see Section S4 in the Supporting Material). We find that the correlation length L_c reaches a sharp maximum near balance where all species are highly correlated (Fig. 2 *C*).

We also computed the susceptibility of the serial network as a function of the input rate λ. We defined the susceptibility in the usual way as the normalized rate of change of the output in response to a small stepwise change of input. The results presented in Section S5 in the Supporting Material show that susceptibility has a strong peak near the balance point, similar to the correlation peak. This gives further evidence that the enzymatic network near balance indeed can be characterized as critical.

We next sought analytical results describing the behavior of this network. For the underloaded regime ($\rho < 1$), it can be rigorously shown that in the absence of dilution ($\gamma = 0$) and in the limit of instant irreversible binding ($\eta^+ \to \infty$, $\eta^- = 0$), the steady-state distribution for $X_1, \ldots, X_n$ in the serial network is the same as that for a parallel network where each of the proteins is produced independently at the rate λ and they all share the same pool of L enzymes that process them (see Section S6 in the Supporting Material). Therefore, in the underloaded regime with no dilution, steady-state same-time correlations among any pair of different proteins in the serial network are the same. From our previous results (13), it follows that the same-time correlation between any two different proteins X_i and X_j is equal to:

$$r_{ij}(\tau = 0) = \frac{F-1}{F-1+n}, \tag{19}$$

where F is the Fano factor (the ratio of the variance to the mean) of the steady-state distribution of the total number of all proteins, $Q = \sum_i Q_i$. The moments of Q and its Fano factor can be found analytically in closed form (13).

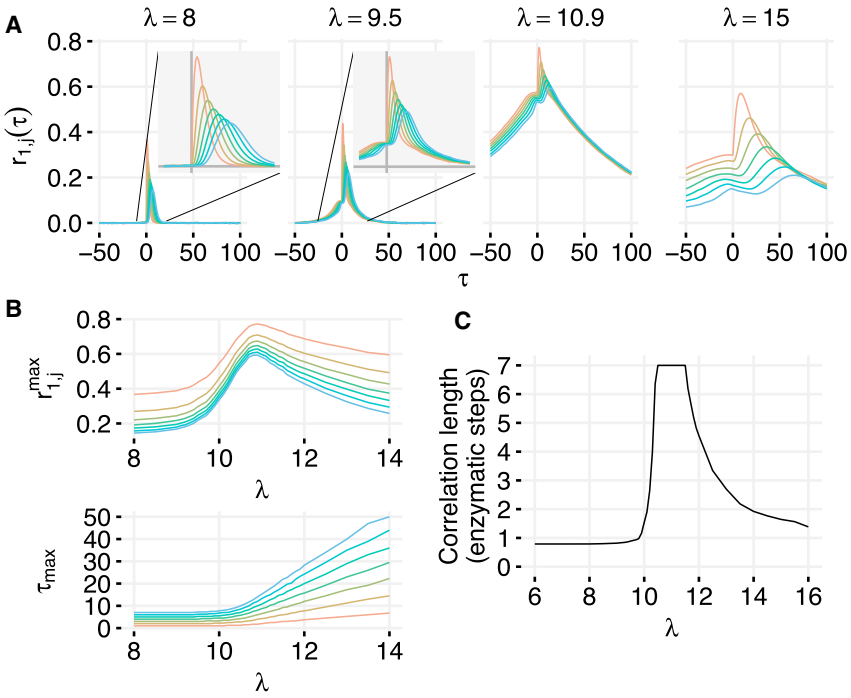

FIGURE 2 (*A*) Time-shifted correlations in different regimes for the serial network with a shared enzyme (see Fig. 1 *B*). The broadening of the $r_{1j}(\tau)$ curves indicates that the correlation time increases as criticality is approached. (*B*) The value of the maximum correlation between $Q1$ and Q_j ($r_{1j}^{\max}$) and the time delay at which that correlation is found ($\tau_{\max}$). In the underloaded regime, the delay is short and correlations are small. Near the balance point, delay increases slightly while correlation increases dramatically. In the overloaded regime, the delay becomes very large and correlations decrease. (*C*) Correlation length in the serial biochemical network with a shared enzyme. Correlation length was calculated as interpolated distance in reaction steps at which $r_{1j}^{\max} = 0.5$ (see Section S4 in the Supporting Material). Parameters for all simulations were $\gamma = 0.01$, $\mu = 1$, $\eta^+ = 1000$, $\eta^- = 0$, and $L = 80$. To see this figure in color, go online.

For $L = 1$, the expressions simplify and $r_{ij} = 1/(1 + n(\rho^{-1} - 1))$. For other values of L, one can obtain the leading term in the Taylor expansion of the correlation for small ρ (strongly underloaded regime), $r_{ij} \approx (\rho L)^L/(L!n) + O[(\rho L)^{L+1}]$. It can also be shown that the correlation r_{ij} approaches 1 as $\rho \to 1$. Fig. 3 *A* demonstrates excellent agreement between our analytical formulae and stochastic simulations.

In the strongly underloaded regime ($\rho << 1$), the enzymatic reactions are approximately first-order (the propensities depend only on the number of proteins and not on the number of enzymes, because free enzymes are nearly always available). Using this approximation, the time-delayed correlations between protein levels are given by

$$r_{1j}(\tau) = \frac{(\mu\tau)^{j-1}}{(j-1)!} e^{-\mu\tau}, \tau > 0, \qquad (20)$$

and are 0 for negative τ-values (see Section S7 in the Supporting Material). For large positive τ, correlations decay exponentially with rate μ. Fig. 3 *B* shows good agreement between this theoretical formula and direct numerical simulations of an eight-stage enzymatic chain. This calculation can be straightforwardly extended to the case of nonzero dilution (see Section S7 in the Supporting Material).

Adaptation in a parallel enzymatic network

The critical behavior of enzymatic networks near the balance point described above is striking, but requires precise tuning of system parameters. However, living organisms employ numerous adaptive strategies to optimize resource allocation in the face of uncertain and variable environmental conditions. Indeed, having too many enzymes to process arriving proteins would be wasteful, while an insufficient number of enzymes would create an excess of unprocessed molecular species. We wondered whether adaptation of enzyme levels would drive the system toward the balance point and lead to the critical state, eliminating the need for parameter tuning.

We performed stochastic simulations of the adaptive system associated with Eq. 6 with two types of proteins and with $\nu = \alpha(Q_1 + Q_2)$. Fig. 4, *C* and *D*, shows the correlations between different proteins, as well as mean enzyme levels, as functions of α. The range of α values that effectively leads to adaptation can be seen as the region where the enzyme level is flat in Fig. 4 *D*. In agreement with the above estimate, for $\gamma = 0.01$ and $\mu = 1$ it spans the range from 10^{-4} to 10^{-2}. Fig. 4 *E* shows the heat maps of the steady-state correlations for different values of λ_1,λ_2 with or without adaptation. While in the nonadaptive case the correlations are high only in the vicinity of the balance line $\lambda_1 + \lambda_2 = \mu$L, in the adaptive cases the correlations are strong through nearly the whole range of synthesis rates. Similarly strong correlation in a broad range of input rates is obtained for other forms of the adaptation function; for example, when the adaptation rate is proportional to the number of unbound proteins of only one kind, $\nu = \alpha Q_1^{\mu}$ (see Section S9 in the Supporting Material).

If the adaptation rate ν depends only on the sum of all protein counts, and the binding of proteins to enzyme is

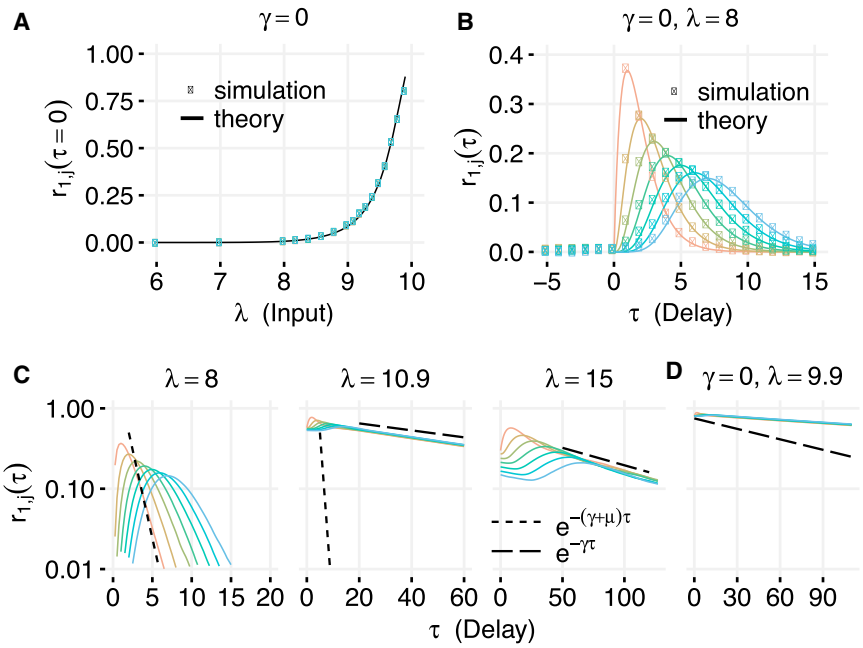

FIGURE 3 Comparison of analytical results to simulation for a serial shared-enzyme network. (*A*) Same-time correlations between species as a function of the input rate λ for the no-dilution network. (*Points*) Correlations from stochastic simulations; (*lines*) correlation predicted using Eq. 19. (*B*) Time-delayed correlations $r_{1j}(\tau)$ in the underloaded regime with no dilution. (*Points*) Correlations from stochastic simulations; (*lines*) correlations predicted from Eq. 20. (*C*) Temporal decay of correlations in different regimes with $\gamma = 0.01$. In the underloaded regime ($\lambda = 8$, *left*), correlations decay as $e^{-(\mu+\gamma)\tau}$. In the overloaded regime ($\lambda = 15$, *right*), they decay as $e^{-\gamma\tau}$. Near balance (*center*), correlation decay slows dramatically, but for nonzero γ cannot decay slower than $e^{-\gamma\tau}$. (*D*) In the absence of dilution, correlations near balance decay very slowly. Vertical scale shared with (*C*). Parameters not shown were $\mu = 1$, $\eta^+ = 1000$, $\eta^- = 0$, and $L = 80$. To see this figure in color, go online.

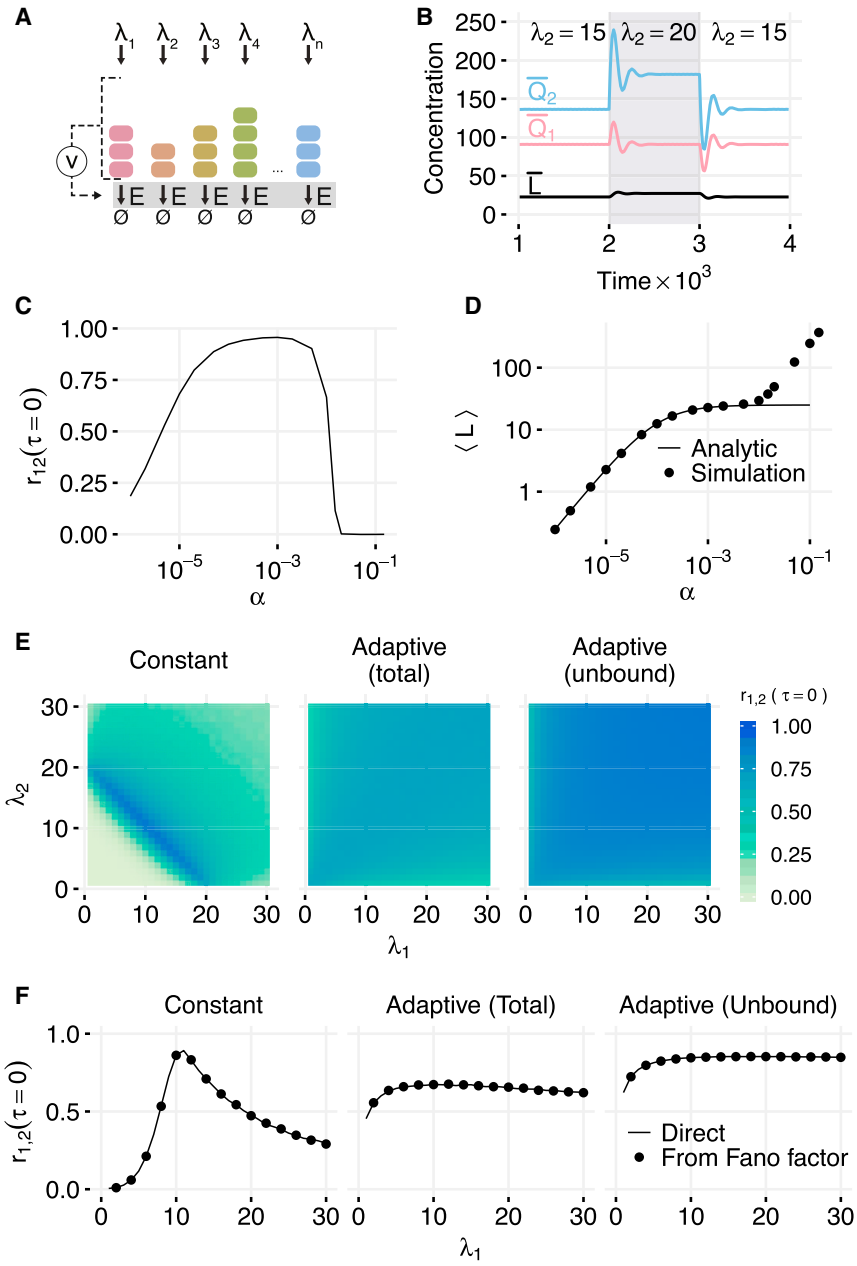

FIGURE 4 Adaptive queueing in a parallel enzymatic network. (*A*) Diagram of the system. (*B*) Perfect adaptation in the deterministic model of the adaptive queueing network with two proteins ($n = 2$) with $\lambda_1 = 10$, $\lambda_2 = 15$, $K_m = 0.1$, $\mu = 1$, $\gamma = 0.01$, and $\alpha = 0.001$. When λ_2 is transiently changed from 15 to 20 (*shaded region*), all species initially respond. The other species $\overline{Q}_1$ then settles to its original steady-state value. (*C*) Dependence of correlation on α in stochastic simulations of a two-species system with $\lambda_1 = 10$, $\lambda_2 = 15$, $\mu = 1$, $\gamma = 0.01$, $\eta^+ = 1000$, and $\eta^- = 0$. Adaptation is effective for α across roughly three orders of magnitude. (*D*) Dependence of $\overline{L}$ (mean enzymes including those bound to proteins) on α in stochastic simulations compared with the analytical expression given in Eq. 11. Mean enzyme level is constant for α in the range that gives effective adaptation. (*E*) Same-time correlations in stochastic simulations for different combinations of λ_1 and λ_2 with $\alpha = 0.01$ and other parameters as in (*C*). In the constant enzyme case (*left*), correlations are only high in the vicinity of the balance line $\lambda_1 + \lambda_2 = 20$. In the systems adapting to either total species (*left*) or unbound species (*right*), correlations are high for nearly all combinations of rates. Same-time correlations are used because the absence of spatial structure in the parallel network removes the delays seen in serial networks. (*F*) Same-time correlations between Q_1 and Q_2 in stochastic simulations of nonadaptive and adaptive networks. Here $\lambda_2 = 10$ with λ_1 varying. For a constant number of enzymes, the correlation peaks near the balance point (*left*); however, when enzyme levels adapt to total number of proteins (*center*) or the number of unbound proteins (*right*), correlations are high for nearly all inputs. (*Lines*) Results of full stochastic simulations of the expressions in Eq. 6. (*Points*) Correlations calculated using Eq. S23 with the Fano factor computed from numerical simulation of the 2D Markov process given in the expressions in Eq. 21. To see this figure in color, go online.

very fast, an extension of the method used in Mather et al. (13) allows us to approximately express the multidimensional steady-state distribution for the protein counts in terms of that for a two-dimensional (2D) birth-death process that tracks the sum Q and the number L of the enzyme copies that are in the system. Under an instant binding assumption, this finding reduces the dimension of the natural Markovian state descriptor from $2n+1$ to 2 and allows us to explore steady-state correlations using numerical methods for the 2D process (Q,L). Furthermore, it can be rigorously shown (see Section S8 in the Supporting Material) that the correlation coefficient $r_{ij}(\tau = 0)$ can still be expressed as a function of the Fano factor of the one-dimensional distribution of the total number of proteins using Eq. 19 when all production rates are equal. For a system with different production rates $\lambda_i \neq \lambda_j$ for $i \neq j$, Eq. S23 (Supporting Material) can be used.

Under the instant binding assumption, the stochastic dynamics of protein X (which denotes any type of protein free or bound to E) and enzyme E (also both free or bound to protein) can be described by the following set of biochemical reactions (where the quantities above the arrows now indicate propensities of the corresponding reactions):

$$\begin{aligned}
&\varnothing \xrightarrow{\Lambda} X,\\
&\varnothing \xrightarrow{\nu(Q)} E,\\
&X \xrightarrow{\mu(Q\wedge L)} \varnothing,\\
&X \xrightarrow{\gamma Q_f} \varnothing,\\
&E \xrightarrow{\gamma L_f} \varnothing,\\
&X + E \xrightarrow{\gamma(Q\wedge L)} \varnothing,
\end{aligned} \tag{21}$$

where Q and L values are the total numbers of protein X and enzyme E at time t, respectively; $(Q\wedge L)$ indicates the smaller of Q and L; and $Q_f = Q - (Q\wedge L)$ and $L_f = L - (Q\wedge L)$ values are the number of unbound copies of protein and enzyme, respectively. The last reaction denotes simultaneous removal of one protein and one enzyme when a protein-enzyme complex is diluted.

This set of reactions describes the dynamics of a 2D nonlinear birth-death process for which the steady-state distribution cannot be found analytically. An approximate solution can be found assuming that the adaptation rate $\nu(Q)$ and dilution rate γ are small compared with protein synthesis and enzymatic degradation rates Λ, μ. In this case, the number of enzymes changes slowly compared with the number of proteins, and the marginal probability distribution for Q equilibrates toward the stationary distribution $P_s(Q\,|\,L)$ corresponding to a fixed value of L (see Mather et al. (13)). The slow dynamics of L can be approximated as a nonlinear birth-death process with the birth rate $\nu(\langle Q\,|\,L\rangle)$ and the death rate γ. In the general case of nonsmall α, we can perform numerical simulations of the reduced 2D birth-death process (Q, L) to compute the Fano factor F and then use Eq. 19 to compute the correlations between Q_1 and Q_2. Fig. 4 *F* compares this method with the results of direct simulations of the system described by Eq. 6. As expected, there is excellent agreement between the two.

Adaptation in serial enzymatic networks

To investigate the statistical properties of the adaptive serial network, we performed direct numerical simulations of the full stochastic model associated with Eq. 13. As with the parallel network, for a broad range of intermediate values of α, the cross correlations between Q_1 and other Q_k are high (Fig. 5 *C*) and nearly identical independent of λ (Fig. 5 *E*). As before, the mean number of enzymes exhibits a plateau in the region of adaptation in excellent agreement with Eq. 18, but for larger $\alpha > \gamma$ deviates up when the Michaelis-Menten approximation loses its validity (Fig. 5 *D*). Interestingly, the temporal cross-correlation functions demonstrate nonmonotonous behavior that is due to stochastic ringing caused by the negative feedback loop. The frequency of ringing is, as expected, dependent on α (Fig. 5 *F*).

We obtained similar results for a network with enzyme synthesis rate proportional to the abundance of the first or the last protein in the series (see Sections S10 and S11 in the Supporting Material). These results show that adaptation and approach to criticality also takes place in these cases; however, in the second case the adaptation is less robust. In particular, it is possible for enzyme production to permanently cease if both E and Q_8 are zero at the same time. However, if we add small basal synthesis of E, adaptation becomes robust again. We also considered the case when ν is proportional to the total abundance of unbound proteins (see Section S12 in the Supporting Material). The latter form of adaptation generated even higher correlations than those using total proteins, because the number of unbound proteins is more sensitive to queueing.

We also computed the network susceptibility to small input perturbations using the deterministic model Eqs. 14–16 (and see Section S5 in the Supporting Material). Again similarly to the cross-correlation analysis, the susceptibility becomes virtually independent of λ because the network adapts to the neighborhood of the balance point. However, generally the susceptibility of the adaptive network is lower than for the nonadaptive one at the balance because of the negative feedback, which is known to reduce the magnitude of the response to external perturbations.

DISCUSSION

Much attention has been given to the question of how cells are able to function reliably when biological networks are seemingly so noisy. Here we used a queueing approach to study a broad class of networks in which protein species are processed by a common enzyme or utilize a common cofactor. Despite the noisiness of the networks' dynamics due to intrinsic stochasticity of the underlying biochemical reactions, we found strong and long-range correlations among multiple protein species near the balance between the substrate input rates and the processing capacity of the network. Furthermore, the correlation time also increases dramatically as the system approaches the balance point. This phenomenology suggests that, at the balance point, enzymatic networks are poised near a critical state.

We also considered network adaptation where the enzyme (or cofactor) synthesis is regulated by the protein species processed by the enzyme. Our theoretical analysis shows that for sufficiently slow adaptation, the network automatically approaches the balance point with large and slowly decaying correlations. An adaptive queueing network therefore behaves much like a self-organized critical system where the critical point is an attractor (39). It is interesting to note that self-organized critical states characterized by a power-law distribution in the abundances of different reactants in random autocatalytic metabolic networks with active transport of nutrients were found in Furusawa and Kaneko (34) and Awazu and Kaneko (40), where this was

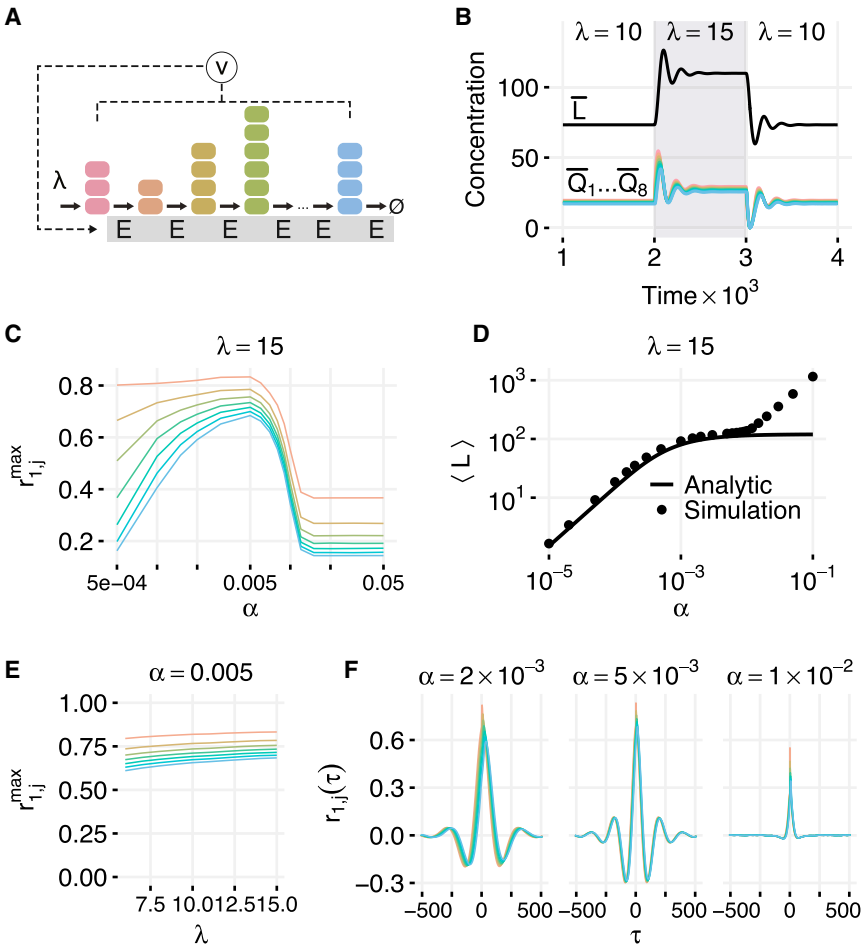

FIGURE 5 Simulations of the adaptive serial enzymatic network. (*A*) Schematic of the adaptive network. The production rate of the enzyme E is set by ν. Here we consider $\nu = \alpha Q$, where Q is the total number of proteins (free and enzyme-bound) in the system. (*B*) Results from a deterministic model of the adaptive queueing system with $\mu = 1$, $\gamma = 0.01$, $\alpha = 0.005$, and $K_m = 0.1$. When the input rate of X_1 is changed, levels of all proteins transiently oscillate before reaching a new steady-state level. (*C*) Maximum correlations between X_1 and X_j as a function of the adaptation parameter α for $\lambda = 15$. For very low α, not enough enzyme is produced and for high α, enough enzyme is produced that the system is always underloaded. (*D*) Mean total enzyme level for different values of α. The range where adaptation occurs can be seen as the flat region of the curve. (*E*) Maximum correlations between X_1 and X_j as a function of λ for $\alpha = 0.005$. (*F*) Correlations as a function of τ for different values of α with $\lambda = 15$. Oscillations increase in strength and frequency for larger α but eventually disappear for high α. In (*C–F*), other simulation parameters are $\mu = 1$, $\gamma = 0.01$, $\eta^+ = 1000$, and $\eta^- = 0$. To see this figure in color, go online.

shown to lead to optimal cell growth. The tendency of adaptive networks to spontaneously approach a critical state may also explain recent experimental observations of criticality in neuronal systems (41) and development (10). The ability of signal transduction cascades to respond to changes in the statistical properties of the input and maximize their information capacity also relies on enzymatic adaptation (30). Taken together with ours, these results point toward the ubiquity and wide-ranging implications of the tendency of enzymatic networks toward criticality.

Emergence of adaptivity of the kind considered here appears to be evolutionarily advantageous, because the balance between the input flux and the processing capacity provides optimal use of enzymatic resources and maximizes cell growth. It can be achieved if one of the species in the queue acts as a transcription factor or posttranscriptional regulator of the limiting enzyme or cofactor synthesis. This motif is in fact observed in natural systems. For example, the *Saccharomyces cerevisiae* transcription factor Rpn4 stimulates production of proteasome genes but is itself degraded by the proteasome (42). In a population context, when overproduction of certain species becomes toxic, the adaptation toward balance may lead to complex, possibly bimodal distributions of cellular phenotypes (6).

The balance point also appears to be optimal for synchronizing levels of the interacting species in a network. In the underloaded regime, changes in protein levels propagate across the network very rapidly, but with low fidelity (small correlations). In the overloaded regime correlations are high, but the delay in their propagation is large. At the balance point, correlations are maximized, while delay times are only slightly increased compared to the underloaded regime. Given the generality of our model and the ubiquity of molecular competition, we anticipate that understanding these more general cases might provide useful insights for whole cell models with many substrates connected by a core of common enzymes and cofactors.

SUPPORTING MATERIAL

Supporting Materials and Methods and 12 figures are available at http://www.biophysj.org/biophysj/supplemental/S0006-3495(16)30616-6.

AUTHOR CONTRIBUTIONS

R.J.W., J.H., and L.S.T. conceived and designed research; P.J.S. and L.S.T. performed and analyzed numerical simulations; and all authors participated in theoretical analysis and contributed to writing the article.

ACKNOWLEDGMENTS

This work was supported by the National Science Foundation and the National Institutes of Health under the Joint DMS/NIGMS Initiative to Support Research at the Interface of the Biological and Mathematical Sciences, National Science Foundation grant No. DMS-1463657, National Science Foundation grant No. DMS-1206772, and the San Diego Center for Systems Biology, National Institutes of Health grant No. P50-GM085764.

REFERENCES

1. Rao, C. V., D. M. Wolf, and A. P. Arkin. 2002. Control, exploitation and tolerance of intracellular noise. *Nature.* 420:231–237.
2. Eldar, A., and M. B. Elowitz. 2010. Functional roles for noise in genetic circuits. *Nature.* 467:167–173.
3. Tsimring, L. S. 2014. Noise in biology. *Rep. Prog. Phys.* 77:026601.
4. Kim, S. Y., and J. E. Ferrell, Jr. 2007. Substrate competition as a source of ultrasensitivity in the inactivation of Wee1. *Cell.* 128:1133–1145.
5. Buchler, N. E., and M. Louis. 2008. Molecular titration and ultrasensitivity in regulatory networks. *J. Mol. Biol.* 384:1106–1119.
6. Ray, J. C. J., M. L. Wickersheim, …, G. Balázsi. 2016. Cellular growth arrest and persistence from enzyme saturation. *PLOS Comput. Biol.* 12:e1004825.
7. Bak, P., and C. Tang. 1989. Earthquakes as a self-organized critical phenomenon. *J. Geophys. Res.* 94:15635–15637.
8. Sneppen, K., P. Bak, …, M. H. Jensen. 1995. Evolution as a self-organized critical phenomenon. *Proc. Natl. Acad. Sci. USA.* 92:5209–5213.
9. Elf, J., J. Paulsson, …, M. Ehrenberg. 2003. Near-critical phenomena in intracellular metabolite pools. *Biophys. J.* 84:154–170.
10. Krotov, D., J. O. Dubuis, …, W. Bialek. 2014. Morphogenesis at criticality. *Proc. Natl. Acad. Sci. USA.* 111:3683–3688.
11. Sauro, H. M. 2012. Enzyme Kinetics for Systems Biology. Future Skill Software, Seattle, WA.
12. Levine, E., and T. Hwa. 2007. Stochastic fluctuations in metabolic pathways. *Proc. Natl. Acad. Sci. USA.* 104:9224–9229.
13. Mather, W. H., N. A. Cookson, …, R. J. Williams. 2010. Correlation resonance generated by coupled enzymatic processing. *Biophys. J.* 99:3172–3181.
14. Cookson, N. A., W. H. Mather, …, J. Hasty. 2011. Queueing up for enzymatic processing: correlated signaling through coupled degradation. *Mol. Syst. Biol.* 7:561.
15. Mather, W. H., J. Hasty, …, R. J. Williams. 2013. Translational cross talk in gene networks. *Biophys. J.* 104:2564–2572.
16. Hochendoner, P., C. Ogle, and W. H. Mather. 2014. A queueing approach to multi-site enzyme kinetics. *Interface Focus.* 4:20130077.
17. Vind, J., M. A. Sørensen, …, S. Pedersen. 1993. Synthesis of proteins in *Escherichia coli* is limited by the concentration of free ribosomes. Expression from reporter genes does not always reflect functional mRNA levels. *J. Mol. Biol.* 231:678–688.
18. Baumgartner, B. L., M. R. Bennett, …, J. Hasty. 2011. Antagonistic gene transcripts regulate adaptation to new growth environments. *Proc. Natl. Acad. Sci. USA.* 108:21087–21092.
19. Mauri, M., and S. Klumpp. 2014. A model for sigma factor competition in bacterial cells. *PLOS Comput. Biol.* 10:e1003845.
20. Yoo, S.-H., J. A. Mohawk, …, J. S. Takahashi. 2013. Competing E3 ubiquitin ligases govern circadian periodicity by degradation of CRY in nucleus and cytoplasm. *Cell.* 152:1091–1105.
21. Prindle, A., J. Selimkhanov, …, J. Hasty. 2014. Rapid and tunable post-translational coupling of genetic circuits. *Nature.* 508:387–391.
22. Figliuzzi, M., E. Marinari, and A. De Martino. 2013. MicroRNAs as a selective channel of communication between competing RNAs: a steady-state theory. *Biophys. J.* 104:1203–1213.
23. Bosia, C., A. Pagnani, and R. Zecchina. 2013. Modelling competing endogenous RNA networks. *PLoS One.* 8:e66609.
24. Babtie, A., N. Tokuriki, and F. Hollfelder. 2010. What makes an enzyme promiscuous? *Curr. Opin. Chem. Biol.* 14:200–207.
25. Cohen, P. 2000. The regulation of protein function by multisite phosphorylation—a 25 year update. *Trends Biochem. Sci.* 25:596–601.
26. Kelly, F. P. 2011. Reversibility and Stochastic Networks. Cambridge University Press, Cambridge, UK.
27. Williams, R. J. 1998. Diffusion approximations for open multiclass queueing networks: sufficient conditions involving state space collapse. *Queueing Syst.* 30:27–88.
28. Bramson, M. 1998. State space collapse with application to heavy traffic limits for multiclass queueing networks. *Queueing Syst.* 30:89–140.
29. Yi, T.-M., Y. Huang, …, J. Doyle. 2000. Robust perfect adaptation in bacterial chemotaxis through integral feedback control. *Proc. Natl. Acad. Sci. USA.* 97:4649–4653.
30. Detwiler, P. B., S. Ramanathan, …, B. I. Shraiman. 2000. Engineering aspects of enzymatic signal transduction: photoreceptors in the retina. *Biophys. J.* 79:2801–2817.
31. El-Samad, H., J. P. Goff, and M. Khammash. 2002. Calcium homeostasis and parturient hypocalcemia: an integral feedback perspective. *J. Theor. Biol.* 214:17–29.
32. Muzzey, D., C. A. Gómez-Uribe, …, A. van Oudenaarden. 2009. A systems-level analysis of perfect adaptation in yeast osmoregulation. *Cell.* 138:160–171.
33. Ni, X. Y., T. Drengstig, and P. Ruoff. 2009. The control of the controller: molecular mechanisms for robust perfect adaptation and temperature compensation. *Biophys. J.* 97:1244–1253.
34. Furusawa, C., and K. Kaneko. 2012. Adaptation to optimal cell growth through self-organized criticality. *Phys. Rev. Lett.* 108:208103.
35. Hatakeyama, T. S., and K. Kaneko. 2014. Kinetic memory based on the enzyme-limited competition. *PLOS Comput. Biol.* 10:e1003784.
36. Gillespie, D. T. 1977. Exact stochastic simulation of coupled chemical reactions. *J. Phys. Chem.* 81:2340–2361.
37. He, F., V. Fromion, and H. V. Westerhoff. 2013. (Im)Perfect robustness and adaptation of metabolic networks subject to metabolic and gene-expression regulation: marrying control engineering with metabolic control analysis. *BMC Syst. Biol.* 7:131.
38. François, P., and E. D. Siggia. 2008. A case study of evolutionary computation of biochemical adaptation. *Phys. Biol.* 5:026009.
39. Bak, P., C. Tang, and K. Wiesenfeld. 1988. Self-organized criticality. *Phys. Rev. A Gen. Phys.* 38:364–374.
40. Awazu, A., and K. Kaneko. 2009. Self-organized criticality of a catalytic reaction network under flow. *Phys. Rev. E Stat. Nonlin. Soft Matter Phys.* 80:010902.
41. Friedman, N., S. Ito, …, T. C. Butler. 2012. Universal critical dynamics in high resolution neuronal avalanche data. *Phys. Rev. Lett.* 108:208102.
42. Xie, Y., and A. Varshavsky. 2001. RPN4 is a ligand, substrate, and transcriptional regulator of the 26S proteasome: a negative feedback circuit. *Proc. Natl. Acad. Sci. USA.* 98:3056–3061.

Biophysical Journal, Volume *111*

Supplemental Information

Criticality and Adaptivity in Enzymatic Networks

Paul J. Steiner, Ruth J. Williams, Jeff Hasty, and Lev S. Tsimring

Criticality and adaptivity in enzymatic networks

Supporting Material

Paul J. Steiner[1], Ruth J. Williams[1,2,*], Jeff Hasty[1,3,4,5,*], Lev S. Tsimring[1,5,*]

[1] BioCircuits Institute, [2] Department of Mathematics, [3] Molecular Biology Section, Division of Biological Sciences, [4] Department of Bioengineering, [5] San Diego Center for Systems Biology, University of California, San Diego, La Jolla, CA 92093

[*] Corresponding authors

1 Serial enzymatic network with reversible binding

Correlation resonance also occurs in enzymatic networks with reversible binding of enzyme to substrate. To demonstrate this, we simulated the serial enzymatic network shown in Figure 1B of the main text with $\eta^+ = 100$, $\eta^- = 10$ (Supp. Fig. S1). We also fixed $\lambda = 10.9$ and varied η^+ and η^- while keeping their ratio fixed at $K_m = \eta^-/\eta^+ = 0.1$ (Supp. Fig.S2).

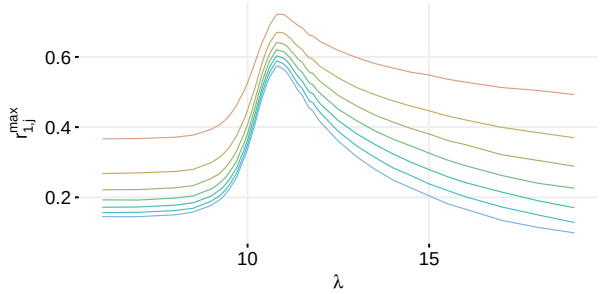

Figure S1: Maximal correlations between X_1 and $X_j, j = 2, ..., 8$ for a serial enzymatic network with reversible binding with $\eta^+ = 100$ and $\eta^- = 10$, giving $K_m = 0.1$. As in Figure 1 of the Main Text, correlation resonance is observed near the balance point $\lambda = 10$, slightly offset by finite dilution rate. Other parameters were $\mu = 1$, $\gamma = 0.01$, and $L = 80$.

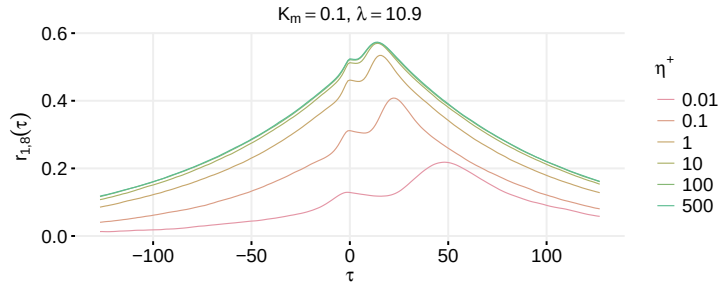

Figure S2: Correlation between X_1 and X_8 as a function of the time delay τ for different η^+ with $K_m = \eta^-/\eta^+$ held constant. The correlations are nearly independent of η^+ for $\eta^+ > 10$, but decrease for very small η^+. Other parameters were $\lambda = 10.9$, $\mu = 1$, $\gamma = 0.01$, and $L = 80$.

2 Parallel enzymatic network with different values of η^+ and η^- for each species

We tested the correlation properties of the parallel 8-node network when binding and unbinding constants of different species to the protease $\eta^\pm$ are different. Our simulations show that the correlation resonance still occurs near the same value of $\lambda \approx \mu L/n$ (see Fig. S3,A), however the magnitudes of the correlation peaks among different species vary significantly. This variability can be explained by the fact that species with higher binding and lower unbinding rate are processed preferentially and more effectively than those that have lower binding and higher unbinding rates because a higher fraction of proteases is bound to them on average. Thus the queues of the former are shorter than of the latter. This is indeed confirmed by the Fig. S3,B where the mean queue lengths $\langle Q_i \rangle$ are plotted against the individual Michaelis constants in the Briggs-Haldane form $K_i = (\mu + \eta_i^-)/\eta_i^+$. Queues with intermediate lengths are closest to criticality and should have higher cross-correlation than very short or very long queues. Figure S3,C indeed shows a strong

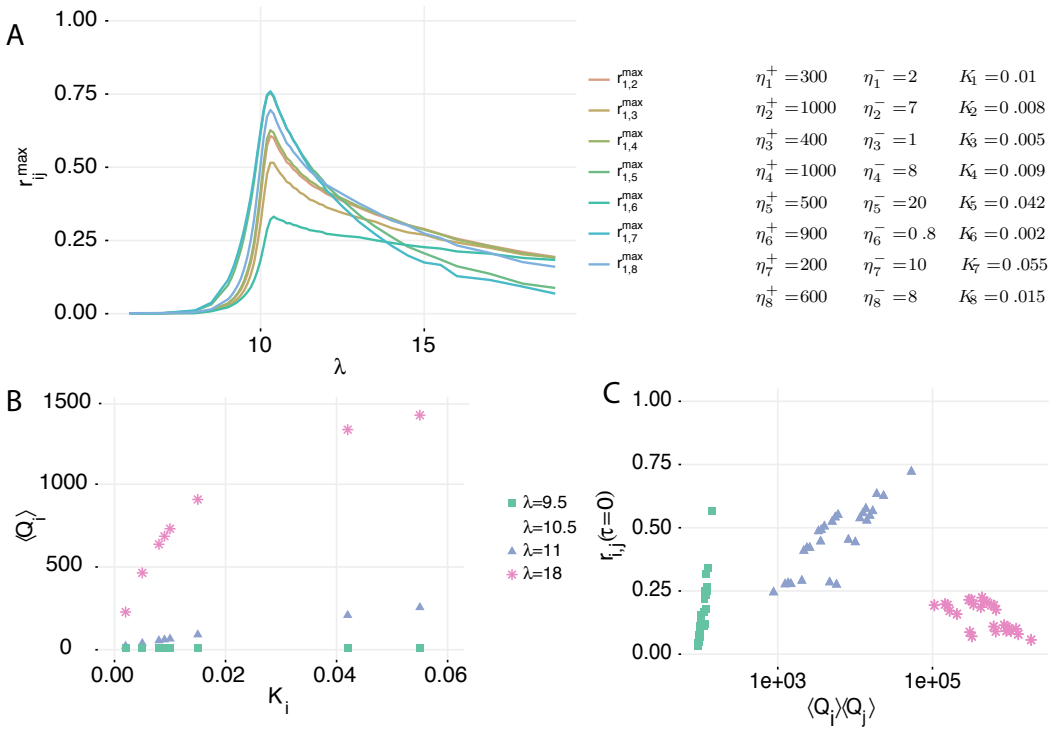

Figure S3: A. Maximum correlations $r_{1,j}^{\max}$ vs. λ in a parallel 8-node network where each protein has different values of η^+ and η^- given on the right together with corresponding $K_i = (\mu + \eta_i^-)/\eta_i^+$. Correlation resonance is still observed near the balance point $\lambda = \mu L/n$, but species with lower K_i have lower cross-correlations near the peak. B. Mean queue lengths of different species $\langle Q_i \rangle$ as functions of K_i. C. Maximum cross-correlation coefficients between different species versus the product of their mean queue lengths for different λ.

correlation between the mean queue lengths and the cross-correlation coefficients with the maximum near $\langle Q_i \rangle \approx 100$.

3 Correlation resonance in a branching network with multiple cofactors

To further test the generality of the correlation resonance phenomenon, we simulated a more complex branching network (Fig. S4A). Rather than a single cofactor, reactions in this network required one of three different cofactors C_1, C_2, C_3 which are assumed to be produced with rates $\lambda_{C_1}, \lambda_{C_2}, \lambda_{C_3}$, respectively. Furthermore, each reaction $X_i + C_k \to X_j$ had its own rate μ_{ij} . Despite these changes, the network still exhibited strong correlation resonance for the subset of species that required the limiting cofactor for processing.

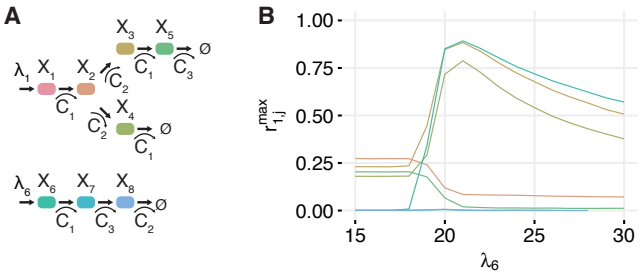

Figure S4: Correlation resonance in a branching network with multiple shared cofactors. (A) A branching network using three different shared cofactors. In this model, each reaction has its own rate rather than all rates being the same. (B) The correlation between a number of species peaks for a particular value of λ_6 with constant $\lambda_1 = 10$. For the parameters used, the cofactor C_1 is limiting, so all species processed by enzymes requiring C_1, *viz.* X_1, X_3, X_4, and X_6, are highly correlated near the balance point. Simulation parameters are $\gamma = 0.01$, $\lambda_{C_1} = \lambda_{C_2} = \lambda_{C_3} = 40$, $\eta^+ = 1000$, $\eta^- = 0$, $\mu_{12} = 1$, $\mu_{23} = 2$, $\mu_{24} = 1$, $\mu_{35} = 3$, $\mu_{4\emptyset} = 1$, $\mu_{5\emptyset} = 2$, $\mu_{67} = 2$, $\mu_{78} = 3$, and $\mu_{8\emptyset} = 2$.

4 Correlation length in a serial enzymatic network

Because the distance between enzymatic "nodes" in the serial network is a discrete variable, we use linear interpolation to define the position along the chain where the maximum correlations drops to $r_0 = 0.5$. For this, suppose $r^{\max}_{1,j+1} \le r_0 < r^{\max}_{1,j}$. Then the correlation length is defined as

$$L_c = j - 1 + \frac{r^{\max}_{1,j} - r_0}{r^{\max}_{1,j} - r^{\max}_{1,j+1}} \tag{S1}$$

When the maximum correlation between the first species and the last species exceeds the threshold (i.e., $r^{\max}_{1,n} > r_0 = 0.5$), the correlation length is assumed to have the maximum possible value $n - 1$.

5 Susceptibility of a serial enzymatic network

We computed the susceptibility of the enzymatic cascade to external perturbations using a deterministic model of an eight-species serial network, Eqs. (14)-(15) of the Main Text with $\bar{L}$ fixed. We switched the input from λ to $\lambda + \Delta\lambda$ for a certain time and computed the changes in $\bar{Q}_i$. The susceptibility is defined as $S_i = \frac{\Delta \bar{Q}_i \lambda}{\bar{Q}_{i0} \Delta\lambda}$, where $\bar{Q}_{i0}$ is the stationary value of $\bar{Q}_i$ at the input rate λ, and $\Delta\bar{Q}_i$ is the maximum change of $\bar{Q}_i$ from the baseline value $\bar{Q}_{i0}$ reached during or after the increase of λ. Similar to the cross-correlation function, the susceptibility as a function of λ exhibits a peak-like shape. For very short pulses, the maximum susceptibility occurs below the balance point. But for longer pulses and for a step function, the maximum susceptibility is achieved very close to the balance point $\lambda = 10$ (figure S5).

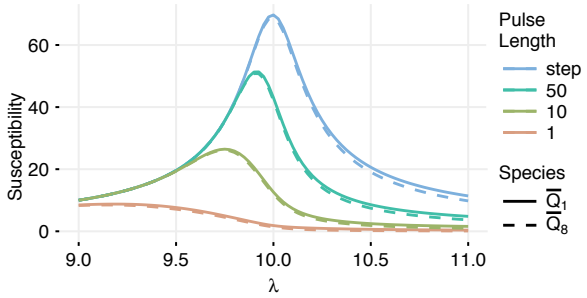

Figure S5: Susceptibility in a deterministic model of a serial enzymatic network of eight species with fixed number of shared enzymes as a function of λ. The value of λ was increased by $\Delta\lambda = 0.1$ for time intervals of length 1, 5, 50, or ∞, and the maximum changes in proteins $\bar{Q}_1, \bar{Q}_8$ were calculated. Parameters used in simulations were $L = 80$, $\gamma = 0.01$, $K_m = 0.1$, $\mu = 1$.

We also computed susceptibility for an adaptive serial network which is described by Eqs. (14)-(16) of the Main Text. Figure S6A shows that the susceptibility becomes nearly independent of λ in analogy with the cross-correlation functions. However, the absolute values of susceptibility become lower. As in stochastic simulations of adaptive networks, for values of α that are small relative to γ, the enzyme synthesis is weak, and the network remains overloaded even with adaptation. For very large α, the feedback is too quick, and the response becomes weak. This produces a trade-off between robustness to changes in λ (due to adaptation) and sensitivity to input signals, which results in an optimal value of adaptation rate α (see Fig. S6B).

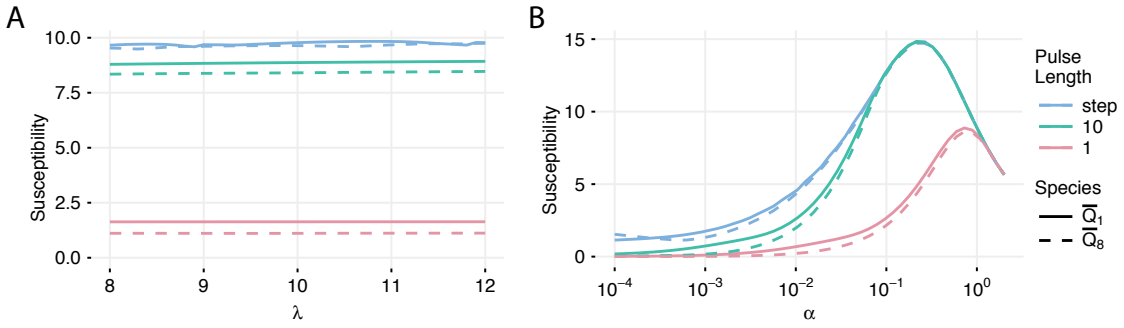

Figure S6: Susceptibility in a deterministic model of an adaptive serial enzymatic network of eight species as a function of λ with $\alpha = 0.05$ (A) and as a function of α for $\lambda = 10$ (B). The value of λ was transiently increased by $\Delta\lambda = 0.1$ for time intervals of length 1, 10, or ∞, and the sensitivity was calculated as described. Parameters used in simulations were $\gamma = 0.01$, $K_m = 0.1$, $\mu = 1$.

6 Steady-state distribution for a serial network with common enzymatic processing

Here we obtain an analytical formula for the steady-state distribution of a Markov chain associated with the serial network with shared enzymatic processing described by the reactions in Eq. 2 of the Main Text, under the instant irreversible binding assumption ($\eta^+ = +\infty, \eta^- = 0$) and in the absence of dilution ($\gamma = 0$).

For $i = 1, \ldots, n$, Q_i^b (resp. Q_i^u) denotes the number of copies of protein X_i that are bound (resp. unbound) to enzyme and L is the (fixed) total number of copies of the enzyme E, whether bound or unbound. The $(2n)$-dimensional process $\mathbf{Q} = (Q_1^u, Q_1^b, \ldots, Q_n^u, Q_n^b)$ is a continuous-time Markov chain. Under our assumptions, we will always have that the total number of bound copies of the proteins is no more than L, i.e., $Q^b = \sum_{i=1}^n Q_i^b \leq L$, and if $Q^b < L$, then $Q^u = 0$. For convenience, we denote the total number of unbound copies of the proteins by $Q^u = \sum_{i=1}^n Q_i^u$ and the total number of copies of all proteins, whether bound or unbound, by $Q = Q^b + Q^u$. We let $\mathcal{Q}$ denote the state space for $\mathbf{Q}$ and $\mathbf{q} = (q_1^u, q_1^b, \ldots, q_n^u, q_n^b)$ will denote a generic value in $\mathcal{Q}$.

We assume that the system is underloaded, i.e., $n\lambda < L\mu$, so that the average load on the enzymatic processing machinery is less than the average processing capacity. Under this assumption, the Markov chain $\mathbf{Q}$ does not explode in finite time, and indeed it will have a unique steady-state distribution.

The infinitesimal generator Γ for $\mathbf{Q}$ is given by the following for $\tilde{\mathbf{q}}, \mathbf{q} \in \mathcal{Q}$:

$$\Gamma(\tilde{\mathbf{q}}, \mathbf{q}) = \begin{cases} \lambda & \text{if } \tilde{\mathbf{q}} = \mathbf{q}^{1,u-} \text{ and } q_1^u > 0, \text{ or} \\ & \quad \text{if } \tilde{\mathbf{q}} = \mathbf{q}^{1,b-} \text{ and } q^u = 0, q_1^b > 0; \\ \mu(q_i^b + 1_{\{i \neq j\}}) \left(\frac{q_j^u + 1_{\{j \neq i+1\}}}{q^u + 1_{\{i=n\}}} \right) & \text{if } \tilde{\mathbf{q}} = \mathbf{q}^{i,b,j,u} \text{ for some } i, j \in \{1, \ldots, n\}, \text{ where} \\ & \quad q_j^b > 0, \ q^b = L \text{ and } \ q_{i+1}^u > 0 \text{ if } i < n; \\ \mu(q_i^b + 1) & \text{if } \tilde{\mathbf{q}} = \mathbf{q}^{i,b,i+1} \text{ for some } i \in \{1, \ldots, n\}, \text{ where} \\ & \quad q^u = 0, \text{ and either } i < n \text{ and } q_{i+1}^b > 0, \\ & \quad \text{or } i = n \text{ and } q^b < L; \\ 0 & \text{for all other } \tilde{\mathbf{q}} \neq \mathbf{q}; \\ -(\lambda + \mu q^b) & \text{if } \tilde{\mathbf{q}} = \mathbf{q}. \end{cases}$$

The off-diagonal entries in Γ indicate the infinitesimal rates for all possible transitions from other states into $\mathbf{q}$. To describe these, let $\mathbf{q} = (q_1^u, q_1^b, \ldots, q_n^u, q_n^b)$ and $q^u = \sum_{i=1}^n q_i^u$, $q^b = \sum_{i=1}^n q_i^b$. The first case in the description of Γ covers transitions associated with production of a new copy of protein X_1. There are two sub-cases to consider, corresponding to the possibilities for the system state $\tilde{\mathbf{q}}$ just before the transition, where in this state, either (i) all copies of the enzyme are bound to copies of the proteins, or (ii) at least one copy of the enzyme is free. For the first sub-case, $\mathbf{q}^{1,u-}$ denotes the modification of $\mathbf{q}$ obtained by subtracting one from q_1^u; note that $q_1^u > 0$ is required for this sub-case to be permissible. For the second sub-case, under our instant binding assumption, a newly produced copy of the protein X_1 will instantly bind to a copy of the enzyme. For this, $\mathbf{q}^{1,b-}$ denotes the modification of $\mathbf{q}$ obtained by subtracting one from q_1^b; note that $q_1^b > 0$ and $q^u = 0$ are required for this sub-case to be permissible. The second and third cases cover transitions due to completion of enzymatic processing of a bound copy of a protein X_i, production of a new unbound copy of protein X_{i+1} (if $i < n$) and instant binding of the freed copy of the enzyme to a copy of some protein (provided there are unbound copies available), where the protein copy is chosen at random from the pool of unbound copies of all of the proteins available just prior to the transition, unless there are no such copies, in which case the enzyme copy binds to the newly produced copy of the protein (if there is one). The second case covers such transitions when there is at least one unbound copy of a protein immediately prior to the transition, and the third case covers transitions in which there are no unbound copies of protein immediately prior to the transition. In the latter case, either a copy of protein X_i for $i < n$ completes its processing and produces a new copy of protein X_{i+1} which instantly binds to the newly freed copy of the enzyme, or a copy of protein X_n completes its processing and a copy of the enzyme becomes free and the total number of proteins shrinks by one. In the second case, assuming $q^u > 0$ or $q^u = 0$, $q^b = L$, $i = n$, the state immediately prior to a transition in which a copy of protein X_i finishes being processed and a copy of protein X_j becomes newly bound, is given by $\mathbf{q}^{i,b,j,u}$. This is obtained from $\mathbf{q}$ by adding one to q_i^b, then subtracting one from q_{i+1}^u if $i < n$, then adding one to q_j^u, and finally, subtracting one from q_j^b. For this transition to be possible, $q_{i+1}^u > 0$ is needed if $i < n$, and $q_j^b > 0$ is needed. For the transitions in the third case, assuming $q^u = 0$ and either $i < n$ or $i = n, q^b < L$, the state immediately prior to a transition, in which a copy of protein X_i finishes being processed, and a copy of protein X_{i+1} is produced and immediately binds to enzyme (if $i < n$), is denoted by $\mathbf{q}^{i,b,i+1}$. This is obtained from $\mathbf{q}$ by adding one to q_i^b and subtracting one from q_{i+1}^b if $i < n$. The latter requires $q_{i+1}^b > 0$.

We now describe the steady-state distribution for $\mathbf{Q}$. For this, given $\mathbf{q} = (q_1^u, q_1^b, \ldots, q_n^u, q_n^b) \in \mathcal{Q}$, $q^u = \sum_{i=1}^n q_i^u$, $q^b = \sum_{i=1}^n q_i^b$, and $q = q^u + q^b$, let

$$\vartheta(\mathbf{q}) \quad = \quad \pi(q)\chi_q(\mathbf{q}), \tag{S2}$$

where

$$\chi_q(\mathbf{q}) \quad = \quad \frac{q^b!}{q_1^b! \cdots q_n^b!} \frac{q^u!}{q_1^u! \cdots q_n^u!} \left(\frac{1}{n} \right)^q \tag{S3}$$

$$\pi(q) \quad = \quad c \frac{(n\lambda)^q}{\prod_{l=1}^q \phi(l)}, \tag{S4}$$

for

$$\phi(l) = \min(l, L)\mu, \tag{S5}$$

$$c^{-1} = \sum_{q=0}^{\infty} \frac{(n\lambda)^q}{\prod_{l=1}^{q} \phi(l)} = \sum_{q=0}^{L-1} \frac{\zeta^q}{q!} + \frac{\zeta^L}{L!(1-\rho)}, \tag{S6}$$

and $\zeta = \frac{n\lambda}{\mu}$, $\rho = \frac{n\lambda}{L\mu} < 1$.

Remark. In the expressions above, x^0 for $x > 0$, $0!$ and a product over an empty set of indices are all defined to equal 1. Also, note that since enzymes will be bound whenever there are sufficiently many copies of proteins to bind to, q^b, q^u can be recovered from q: $q^b = \min(q, L)$ and $q^u = (q - L)^+$.

Theorem 6.1. *Assuming $n\lambda < L\mu$, the probability distribution ϑ is the unique steady-state distribution for* $\mathbf{Q}$. *In other words, in steady-state, the distribution for Q is the same as that for the birth-death process describing the total number of molecules in an L-server first-come-first-served queue with Poisson arrivals at rate $n\lambda$, independent exponentially distributed service times with a mean of $1/\mu$, and, conditioned on Q, the distribution of the protein types is as if each molecule in the system, whether bound or unbound, independently chooses its type, where the probability that it chooses type i is $\frac{1}{n}$, $i = 1, \ldots, n$.*

Remark. It turns out that the steady-state distribution for $\mathbf{Q}$ is the same as for the enzymatic processing model in [4] when the different types of proteins there are all produced independently at rate λ and the dilution parameter γ is set to zero. Our result is almost a special case of a result for multi-class queueing networks described in Corollary 3.5 of Kelly [3]. However, the derivation in Kelly does not allow for immediate feedback to a queue as we have here. One can think of our result as a formal "limit" of Kelly's result for a two-station queueing network, in which the first station is an enzymatic processing queue and the second station is a quick service station that quickly returns a newly produced copy of protein to the enzymatic processing queue. The "limit" is as this quick service time tends to zero. Alternatively, as suggested in Exercise 5 on page 64 of Kelly [3], one can try to extend Kelly's result to a single queue with immediate feedback. That is what we do here. We note however, that for this to be true, it is important for the proof that an enzyme does not immediately bind to the copy of protein that it just produced, unless there are no other copies of protein to bind to. In other words, a newly produced copy of protein is not inserted into the queue of waiting proteins until after the freed enzyme tries to select from the pool of waiting proteins. Only if the pool is empty, does the enzyme bind to the protein just produced.

Proof. Since the Markov chain associated with $\mathbf{Q}$ is irreducible and does not explode in finite time, it suffices to show that ϑ given by (S2) satisfies the following equation (see Theorems 3.5.3 and 3.5.5 of [6]):

$$\sum_{\tilde{\mathbf{q}} \in \mathcal{Q}} \vartheta(\tilde{\mathbf{q}}) \Gamma(\tilde{\mathbf{q}}, \mathbf{q}) = 0 \quad \text{for all } \mathbf{q} \in \mathcal{Q}. \tag{S7}$$

We now verify this. In the following, in the first equality, for the sums over i and j, any term for which $\mathbf{q}^{i,b,j,u}$ or $\mathbf{q}^{i,b,i+1}$ is not in $\mathcal{Q}$ is considered to be zero. Also, indicator functions are suppressed when they

are not needed, e.g., due to the factor multiplying them being zero. For any $\mathbf{q} \in \mathcal{Q}$,

$$
\begin{aligned}
&\sum_{\tilde{\mathbf{q}} \in \mathcal{Q}} \vartheta(\tilde{\mathbf{q}}) \Gamma(\tilde{\mathbf{q}}, \mathbf{q}) \\
&= (\vartheta(\mathbf{q}^{1,u-}) 1_{\{q_1^u > 0\}} + \vartheta(\mathbf{q}^{1,b-}) 1_{\{q^u = 0, q_1^b > 0\}}) \lambda \\
&\quad + 1_{\{q^u > 0\}} \sum_{i=1}^{n} \sum_{j=1}^{n} \vartheta(\mathbf{q}^{i,b,j,u}) \mu(q_i^b + 1_{\{i \neq j\}}) \left(\frac{q_j^u + 1_{\{j \neq i+1\}}}{q^u + 1_{\{i=n\}}} \right) \\
&\quad + 1_{\{q^u = 0, q^b = L\}} \mu \left(\sum_{i=1}^{n-1} \vartheta(\mathbf{q}^{i,b,i+1})(q_i^b + 1)) + \sum_{j=1}^{n} \vartheta(\mathbf{q}^{n,b,j,u})(q_n^b + 1_{\{j \neq n\}}) \right) \\
&\quad + 1_{\{q^b < L\}} \mu \sum_{i=1}^{n} \vartheta(\mathbf{q}^{i,b,i+1})(q_i^b + 1) \\
&\quad - \vartheta(\mathbf{q})(\lambda + \mu q^b) \\
&= \lambda \pi(q-1) (\chi_{q-1}(\mathbf{q}^{1,u-}) 1_{\{q_1^u > 0\}} + \chi_{q-1}(\mathbf{q}^{1,b-}) 1_{\{q^u = 0, q_1^b > 0\}}) \\
&\quad + 1_{\{q^u > 0\}} \frac{\mu \pi(q)}{q^u} \sum_{i=1}^{n-1} \Big(\sum_{j \neq i, i+1} 1_{\{q_j^b > 0, q_{i+1}^u > 0\}} \chi_q(\mathbf{q}^{i,b,j,u})(q_i^b + 1)(q_j^u + 1) \\
&\qquad + 1_{\{q_{i+1}^u > 0\}} \chi_q(\mathbf{q}^{i,b,i,u}) q_i^b (q_i^u + 1) + 1_{\{q_{i+1}^b > 0\}} \chi_q(\mathbf{q}^{i,b,i+1,u})(q_i^b + 1) q_{i+1}^u \Big) \\
&\quad + 1_{\{q^u > 0\}} \frac{\mu \pi(q+1)}{q^u + 1} \Big(\sum_{j \neq n} 1_{\{q_j^b > 0\}} \chi_{q+1}(\mathbf{q}^{n,b,j,u})(q_n^b + 1)(q_j^u + 1) + \chi_{q+1}(\mathbf{q}^{n,b,n,u}) q_n^b (q_n^u + 1) \Big) \\
&\quad + 1_{\{q^u = 0, q^b = L\}} \mu \pi(q) \sum_{i=1}^{n-1} 1_{\{q_{i+1}^b > 0\}} \chi_q(\mathbf{q}^{i,b,i+1})(q_i^b + 1) \\
&\quad + 1_{\{q^u = 0, q^b = L\}} \mu \pi(q+1) \left(\sum_{j=1}^{n-1} 1_{\{q_j^b > 0\}} \chi_{q+1}(\mathbf{q}^{n,b,j,u})(q_n^b + 1) + \chi_{q+1}(\mathbf{q}^{n,b,n,u}) q_n^b \right) \\
&\quad + 1_{\{q^b < L\}} \mu \left(\pi(q) \sum_{i=1}^{n-1} 1_{\{q_{i+1}^b > 0\}} \chi_q(\mathbf{q}^{i,b,i+1})(q_i^b + 1) + \pi(q+1) \chi_{q+1}(\mathbf{q}^{n,b,n+1})(q_n^b + 1) \right) \\
&\quad - \pi(q) \chi_q(\mathbf{q})(\lambda + \mu q^b) \\
&= \lambda \pi(q-1) \chi_q(\mathbf{q}) n \left(\frac{q_1^u}{q^u} 1_{\{q_1^u > 0\}} + \frac{q_1^b}{q^b} 1_{\{q^u = 0, q_1^b > 0\}} \right) \\
&\quad + 1_{\{q^u > 0\}} \frac{\mu \pi(q) \chi_q(\mathbf{q})}{q^u} \sum_{i=1}^{n-1} \Big(\sum_{j \neq i, i+1} q_j^b q_{i+1}^u + q_{i+1}^u q_i^b + q_{i+1}^b q_{i+1}^u \Big) \\
&\quad + 1_{\{q^u > 0\}} \frac{\mu \pi(q+1) \chi_q(\mathbf{q})}{n} \Big(\sum_{j \neq n} q_j^b + q_n^b \Big) \\
&\quad + 1_{\{q^u = 0, q^b = L\}} \mu \chi_q(\mathbf{q}) \left(\pi(q) \sum_{i=1}^{n-1} q_{i+1}^b + \frac{\pi(q+1)}{n} \left(\sum_{j=1}^{n-1} 1_{\{q_j^b > 0\}} q_j^b + q_n^b \right) \right) \\
&\quad + 1_{\{q^b < L\}} \mu \chi_q(\mathbf{q}) \left(\pi(q) \sum_{i=1}^{n-1} 1_{\{q_{i+1}^b > 0\}} q_{i+1}^b + \frac{\pi(q+1)}{n} (q^b + 1) \right) \\
&\quad - \pi(q) \chi_q(\mathbf{q})(\lambda + \mu q^b)
\end{aligned}
$$

$$
\begin{aligned}
&= \pi(q)\chi_q(\mathbf{q})\phi(q)\left(\frac{q_1^u}{q^u}1_{\{q_1^u>0\}} + \frac{q_1^b}{q^b}1_{\{q^u=0,q_1^b>0\}}\right)\\
&\quad +1_{\{q^u>0\}}\frac{\mu\pi(q)\chi_q(\mathbf{q})q^b}{q^u}\left(\sum_{i=1}^{n-1} q_{i+1}^u + \frac{\lambda}{\phi(q+1)}q^u\right)\\
&\quad +1_{\{q^u=0,q^b=L\}}\mu\pi(q)\chi_q(\mathbf{q})\Big(q^b - q_1^b + \frac{\lambda}{\phi(q+1)}q^b\Big)\\
&\quad +1_{\{q^b<L\}}\mu\pi(q)\chi_q(\mathbf{q})\Big(q^b - q_1^b + \frac{\lambda}{\phi(q+1)}(q^b+1)\Big)\\
&\quad -\pi(q)\chi_q(\mathbf{q})(\lambda+\mu q^b)\\
&= \mu\pi(q)\chi_q(\mathbf{q})\Bigg(L\frac{q_1^u}{q^u}1_{\{q_1^u>0\}} + q_1^b 1_{\{q^u=0\}} + 1_{\{q^u>0\}}\left(L\frac{q^u-q_1^u}{q^u}+\frac{\lambda}{\mu}\right)\\
&\qquad\qquad +1_{\{q^u=0,q^b=L\}}\left(q^b - q_1^b + \frac{\lambda}{\mu}\right) + 1_{\{q^b<L\}}\Big(q^b - q_1^b + \frac{\lambda}{\mu}\Big) - \Big(\frac{\lambda}{\mu}+q^b\Big)\Bigg)\\
&= 0.
\end{aligned}
$$

In the above derivation, we have used the forms of π and χ in deriving the string of equalities. In particular, we have used the fact that $\frac{\pi(q+1)}{n} = \frac{\lambda}{\phi(q+1)}\pi(q)$ and that $\phi(q+1) = L\mu$ when $q^u > 0$ or $q^u = 0$, $q^b = L$, and $\phi(q+1) = (q^b+1)\mu$ when $q^b < L$. □

The preceding result leads to the following formulas for the steady-state moments of the total number of copies of protein i, $Q_i = Q_i^u + Q_i^b$, in terms of those for the total number of copies of all proteins, Q. Here overline denotes the mean value, SCV indicates the squared coefficient of variation (the variance divided by the square of the mean), and Var denotes the variance.

Corollary 6.1. *Suppose that the assumptions of Theorem 6.1 hold. Then, in steady-state we have the following for $i = 1, \ldots, n$,*

$$
\begin{aligned}
\overline{Q}_i &= \frac{\overline{Q}}{n}, &\text{(S8)}\\
SCV(Q_i) &= SCV(Q) - \frac{1}{\overline{Q}} + \frac{1}{\overline{Q}_i}, &\text{(S9)}
\end{aligned}
$$

and the steady-state correlation between Q_i and Q_j for $j \neq i$ is given by

$$
\begin{aligned}
r_{ij}(\tau=0) &= \frac{\overline{Q_iQ_j} - \overline{Q}_i\overline{Q}_j}{\sqrt{Var(Q_i)Var(Q_j)}}\\
&= \frac{F-1}{F-1+n}, &\text{(S10)}
\end{aligned}
$$

where $F = Var(Q)/\overline{Q}$ is the steady-state Fano factor for Q.

Proof. From Theorem 6.1, we know that conditioned on $Q = q$, since $q^b = \min(q, L)$ and $q^u = (q-L)^+$, $Q_i^b, i = 1, \ldots, n$, have a multinomial distribution with parameters $(\min(q, L); p_1, \ldots, p_n)$, independent of $Q_i^u, i = 1, \ldots, n$, which have a multinomial distribution with parameters $((q-L)^+; p_1, \ldots, p_n)$, and hence $Q_i, i = 1, \ldots, n$ have a multinomial distribution with parameters $(q; p_1, \ldots, p_n)$, where $p_i = \frac{1}{n}$ for $i = 1, \ldots, n$. The formulas for the moments and correlations of the Q_i, expressed in terms of the moments of Q, then follow from computations using the multinomial distributions. These computations are very similar to those performed in [4]. We leave the details to the reader. □

Formulas for the steady-state moments of Q, which are the steady-state moments for a one-dimensional birth-death process that describes the total number of jobs in an $M/M/L$ queue with arrival rate $n\lambda$ and

service rate μ, can be readily computed. In particular, the following formula for the steady-state mean for Q is from (2.29) in [2]. Here $\zeta = \frac{n\lambda}{\mu}$, $\rho = \frac{n\lambda}{L\mu}$ and c is the normalizing constant for the steady-state distribution of Q, as before.

$$\overline{Q} \;=\; \zeta + c\frac{\zeta^L \rho}{L!(1-\rho)^2},$$

and the second moment can be obtained using the sum of the geometric series of powers of ρ and derivatives thereof as follows:

$$\overline{Q^2} \;=\; c\left\{\sum_{q=1}^{L-1}\frac{q\zeta^q}{(q-1)!} + \frac{\zeta^L}{L!}\left(\frac{2\rho^2}{(1-\rho)^3} + \frac{(2L+1)\rho}{(1-\rho)^2} + \frac{L^2}{1-\rho}\right)\right\}.$$

7 Correlations in a serial enzymatic network below balance

We approximate the underloaded regime by the situation where the number of enzymes is truly unlimited and they bind their substrates infinitely quickly (the strong binding approximation). In this situation, all proteins are always bound to enzymes and the master equation is

$$\begin{aligned}\frac{d}{dt}P(\mathbf{q},t) &= \lambda[P(\mathbf{q}_1,t) - P(\mathbf{q},t)] \\ &+\mu\sum_{i=1}^{n}[(q_i+1)P(\mathbf{q}^i_{i+1},t) - q_i P(\mathbf{q},t)] \\ &+\gamma\sum_{i=1}^{n}[(q_i+1)P(\mathbf{q}^i,t) - q_i P(\mathbf{q},t)]\end{aligned} \tag{S11}$$

where $\mathbf{q}$ stands for a vector of numbers of substrates $(q_1,...,q_n)$. The subscript i in $\mathbf{q}_i$ or $\mathbf{q}^j_i$ indicates that the i-th component of $\mathbf{q}$ (if $i \in \{1,...,n\}$) is replaced by $q_i - 1$, and the superscript j in $\mathbf{q}^j$ or q^j_i means that q_j (if $j \in \{1,...,n\}$) is replaced by $q_j + 1$. For example, $\mathbf{q}^1_2$ denotes the vector $(q_1+1, q_2-1, q_3, ..., q_n)$.

From this master equation, it is straightforward to derive expressions for the steady-state means $\overline{Q}_i$ and same-time covariances $\mathrm{cov}(Q_i,Q_j) = \overline{Q_iQ_j} - \overline{Q}_i\overline{Q}_j$,

$$\overline{Q}_i = \frac{\alpha\mu^{i-1}}{(\mu+\gamma)^i} \tag{S12}$$

$$\mathrm{cov}(Q_i,Q_j) = \overline{Q}_i\delta_{i,j} \tag{S13}$$

where $\delta_{i,j}$ is the Kronecker symbol.

For a system of only zero- and first-order Markovian reactions, the regression theorem dictates that the time-delayed covariance is given by (see [1])

$$\mathrm{cov}(\mathbf{Q}(t),\mathbf{Q}(t+\tau)) = e^{\mathbf{B}\tau}\overline{\tilde{\mathbf{Q}}(t)\tilde{\mathbf{Q}}^T(t)} \tag{S14}$$

where $\mathbf{B}$ is the Jacobian of the corresponding linear system for the means, $\overline{\mathbf{Q}} = -\mathbf{B}^{-1}\mathbf{A}$, and $\tilde{\mathbf{Q}} = \mathbf{Q} - \overline{\mathbf{Q}}$.

For this system the Jacobian $\mathbf{B}$ has the bi-diagonal form

$$\mathbf{B} = \begin{pmatrix} -\mu-\gamma & 0 & 0 & \dots & 0 \\ \mu & -\mu-\gamma & 0 & \dots & 0 \\ 0 & \mu & -\mu-\gamma & \dots & 0 \\ \vdots & \vdots & \vdots & \ddots & \vdots \\ 0 & 0 & 0 & \mu & -\mu-\gamma \end{pmatrix} \tag{S15}$$

Since $\mathbf{B}$ is a sum of commuting diagonal matrix $\mathbf{B}_0$ with elements $-(\mu+\gamma)\delta_{i,j}$ and the lower shift matrix $\mathbf{L}$ with elements $\mu\delta_{i,j+1}$, the matrix exponential $\exp(\mathbf{B}\tau)$ can be written as

$$\exp(\mathbf{B}\tau) = e^{-(\mu+\gamma)\tau}\left(\mathbf{I} + \mathbf{L}\tau + \frac{1}{2}\mathbf{L}^2\tau^2 + \ldots + \frac{1}{(n-1)!}\mathbf{L}^{n-1}\tau^{n-1}\right) \tag{S16}$$

Taking advantage of the properties of powers of shift matrices, we can easily compute the covariance

$$\mathrm{cov}(Q_1(t), Q_j(t+\tau)) = \frac{\mu^{j-1}\tau^{j-1}}{(j-1)!}\frac{\alpha}{\mu+\gamma}e^{-(\mu+\gamma)\tau} \tag{S17}$$

Then the expression for the correlation coefficient between $Q_1(t)$ and $Q_j(t+\tau)$ is

$$r_{1j}(\tau) = \frac{[\mu(\mu+\gamma)]^{\frac{j-1}{2}}\tau^{j-1}}{(j-1)!}e^{-(\mu+\gamma)\tau}. \tag{S18}$$

8 Factorized steady-state distributions for a parallel network with adaptive enzymatic processing

Here we establish a factorization result for the steady-state distribution of the $(2n+1)$-dimensional Markov chain associated with the parallel network with shared enzymatic processing and adaptation described by Eq. 8 in the Main Text. Under irreversible, instant binding ($\eta_- = 0, \eta_+ = +\infty$), when the adaptation rate ν depends only on the sum of all protein counts, this means that the steady-state correlation coefficient r_{ij} (for $\tau = 0$) can be computed from the steady-state distribution for the two-dimensional Markov chain associated with the total number of protein copies and the total number of copies of the enzyme.

For $i = 1, \ldots, n$, we let Q_i^b (resp. Q_i^u) denote the number of copies of protein X_i that are bound (resp. unbound) to enzyme and let L denote the total number of copies of the enzyme E, whether bound or unbound. Note that L is no longer constant, it is a stochastic process. Let $Q^b = \sum_{i=1}^n Q_i^b$ and $Q^u = \sum_{i=1}^n Q_i^u$, the total number of copies of bound and unbound protein, respectively, and let $Q = Q^b + Q^u$, the total number of copies of all proteins, whether bound or unbound. Note that since L denotes the total number of copies of the enzyme (bound plus unbound), we will always have that the total number of bound copies of proteins is no more than L, i.e., $Q^b \leq L$. We assume that ν is a measurable function of (Q^u, Q^b, L), in particular, this covers the case where ν just depends on Q. The $(2n+1)$-dimensional process

$$\mathbf{Z} = (Q_1^u, Q_1^b, \ldots, Q_n^u, Q_n^b, L)$$

is a continuous-time Markov chain. We let $\mathcal{Z}$ denote the state space for $\mathbf{Z}$ and $\mathbf{z} = (q_1^u, q_1^b, \ldots, q_n^u, q_n^b, \ell)$ will denote a generic value in $\mathcal{Z}$. In addition, because of our assumptions that η^+, η^-, μ and γ do not depend on i, and that ν depends only on (Q^u, Q^b, L), we have that the three-dimensional process

$$\mathbf{W} = (Q^u, Q^b, L)$$

is a continuous-time Markov chain. We denote the state space for $\mathbf{W}$ by $\mathcal{W}$ and a generic element of this space by $\mathbf{w} = (q^u, q^b, \ell)$.

We assume that the function ν is such that $\mathbf{Z}$ is irreducible and does not explode in finite time and is such that $\mathbf{W}$ has a steady-state distribution. Then $\mathbf{Z}$ has a unique steady-state distribution. We will show that the steady-state distribution for $\mathbf{Z}$ can be expressed in terms of that for $\mathbf{W}$.

The infinitesimal generator for $\mathbf{Z}$ is given by the following for $\tilde{\mathbf{z}}, \mathbf{z} \in \mathcal{Z}$:

$$\Gamma(\tilde{\mathbf{z}}, \mathbf{z}) = \begin{cases} \lambda_i & \text{if } \tilde{\mathbf{z}} = \mathbf{z}^{i,u-} \text{ for some } i \in \{1, \ldots, n\} \text{ and } q_i^u > 0, \\ \gamma(q_i^u + 1) & \text{if } \tilde{\mathbf{z}} = \mathbf{z}^{i,u+} \text{ for some } i \in \{1, \ldots, n\}, \\ \eta^+(\ell - q^b + 1)(q_i^u + 1) & \text{if } \tilde{\mathbf{z}} = \mathbf{z}^{i,u+,b-} \text{ for some } i \in \{1, \ldots, n\} \text{ and } q_i^b > 0, \\ \eta^-(q_i^b + 1) & \text{if } \tilde{\mathbf{z}} = \mathbf{z}^{i,u-,b+} \text{ for some } i \in \{1, \ldots, n\} \text{ and } q_i^u > 0, \\ \mu(q_i^b + 1) & \text{if } \tilde{\mathbf{z}} = \mathbf{z}^{i,b+} \text{ for some } i \in \{1, \ldots, n\}, \\ \gamma(q_i^b + 1) & \text{if } \tilde{\mathbf{z}} = \mathbf{z}^{i,b+,\ell+} \text{ for some } i \in \{1, \ldots, n\}, \\ \nu(q^u, q^b, \ell - 1) & \text{if } \tilde{\mathbf{z}} = \mathbf{z}^{\ell-} \text{ and } \ell > 0, \\ \gamma(\ell - q^b + 1) & \text{if } \tilde{\mathbf{z}} = \mathbf{z}^{\ell+}, \\ 0 & \text{for all other } \tilde{\mathbf{z}} \neq \mathbf{z}, \\ -(\Lambda + \gamma(q^u + \ell) & \\ \quad + \mu q^b + \eta^+ q^u(\ell - q^b) & \\ \quad + \eta^- q^b + \nu(q^u, q^b, \ell)) & \text{if } \tilde{\mathbf{z}} = \mathbf{z}. \end{cases}$$

The off-diagonal entries in Γ indicate the infinitesimal rates for all possible transitions from other states into $\mathbf{z}$. To describe these, let $\mathbf{z} = (\mathbf{q}, \ell)$ for $\mathbf{q} = (q_1^u, q_1^b, \ldots, q_n^u, q_n^b)$, and let $q^u = \sum_{i=1}^n q_i^u$, $q^b = \sum_{i=1}^n q_i^b$. The first case in the description of Γ covers transitions associated with production of a new copy of a protein. For this, $\mathbf{z}^{i,u-}$ denotes the modification of $\mathbf{z}$ obtained by subtracting one from q_i^u. Note that $q_i^u > 0$ is needed for this transition to be possible. The second case covers transitions due to dilution of an unbound copy of a protein. For this, $\mathbf{z}^{i,u+}$ denotes the modification of $\mathbf{z}$ obtained by adding one to q_i^u. The third case covers transitions due to binding of an unbound copy of a protein to an unbound copy of the enzyme. For this, $\mathbf{z}^{i,u+,b-}$ denotes the modification of $\mathbf{z}$ obtained by adding one to q_i^u and subtracting one from q_i^b, and $\ell - q^b + 1$ is the number of unbound copies of the enzyme associated with $\mathbf{z}^{i,u+,b-}$. The fourth case covers transitions due to unbinding of a copy of a protein bound to a copy of the enzyme. For this, $\mathbf{z}^{i,u-,b+}$ denotes the modification of $\mathbf{z}$ obtained by subtracting one from q_i^u and adding one to q_i^b. The fifth case covers transitions due to completion of enzymatic degradation of a bound copy of a protein. For this, $\mathbf{z}^{i,b+}$ denotes the modification of $\mathbf{z}$ obtained by adding one to q_i^b. The sixth case covers transitions due to dilution of a copy of a protein bound to a copy of the enzyme. For this, $\mathbf{z}^{i,b+,\ell+}$ denotes the modification of $\mathbf{z}$ obtained by adding one to q_i^b and to ℓ. The seventh case covers a transition due to production of a new copy of the enzyme. For this, $\mathbf{z}^{\ell-}$ denotes the modification of $\mathbf{z}$ obtained by subtracting one from ℓ. The eighth case covers a transition due to dilution of an unbound copy of the enzyme. For this, $\mathbf{z}^{\ell+}$ denotes the modification of $\mathbf{z}$ obtained by adding one to ℓ.

The infinitesimal generator for $\mathbf{W}$ is given by the following for $\tilde{\mathbf{w}}, \mathbf{w} \in \mathcal{W}$:

$$\Delta(\tilde{\mathbf{w}}, \mathbf{w}) = \begin{cases} \Lambda & \text{if } \tilde{\mathbf{w}} = \mathbf{w}^{u-} \text{ and } q^u > 0, \\ \gamma(q^u + 1) & \text{if } \tilde{\mathbf{w}} = \mathbf{w}^{u+}, \\ \eta^+(\ell - q^b + 1)(q^u + 1) & \text{if } \tilde{\mathbf{w}} = \mathbf{w}^{u+,b-} \text{ and } q^b > 0, \\ \eta^-(q^b + 1) & \text{if } \tilde{\mathbf{w}} = \mathbf{w}^{u-,b+} \text{ and } q^u > 0, \\ \mu(q^b + 1) & \text{if } \tilde{\mathbf{w}} = \mathbf{w}^{b+}, \\ \gamma(q^b + 1) & \text{if } \tilde{\mathbf{w}} = \mathbf{w}^{b+,\ell+}, \\ \nu(q^u, q^b, \ell - 1) & \text{if } \tilde{\mathbf{w}} = \mathbf{w}^{\ell-} \text{ and } \ell > 0, \\ \gamma(\ell - q^b + 1) & \text{if } \tilde{\mathbf{w}} = \mathbf{w}^{\ell+}, \\ 0 & \text{for all other } \tilde{\mathbf{w}} \neq \mathbf{w}, \\ -\left(\Lambda + \gamma(q^u + \ell)\right. & \\ \quad + \mu q^b + \eta^+ q^u(\ell - q^b) & \\ \quad \left. + \eta^- q^b + \nu(q^u, q^b, \ell)\right) & \text{if } \tilde{\mathbf{w}} = \mathbf{w}. \end{cases} \tag{S19}$$

Here $\Lambda = \sum_{i=1}^n \lambda_i$. The cases for $\Delta(\tilde{\mathbf{w}}, \mathbf{w})$, $\tilde{\mathbf{w}} \neq \mathbf{w}$, correspond to the possible transitions into $\mathbf{w}$. Writing

$\mathbf{w} = (q^u, q^b, \ell)$, these can be described as follows. The first case corresponds to a transition due to production of a new copy of a protein. For this, $\mathbf{w}^{u-}$ denotes the modification of $\mathbf{w}$ obtained by subtracting one from q^u. The second, sixth and eighth cases correspond to transitions due to dilution of an unbound copy of a protein, a protein-enzyme complex or an unbound copy of the enzyme, respectively. For this, $\mathbf{w}^{u+}$ denotes the modification of $\mathbf{w}$ obtained by adding one to q^u, $\mathbf{w}^{b+,\ell+}$ denotes the modification of $\mathbf{w}$ obtained by adding one to q^b and to ℓ, and $\mathbf{w}^{\ell+}$ denotes the modification of $\mathbf{w}$ obtained by adding one to ℓ. The third and fourth cases correspond to transitions due to binding and unbinding of a copy of a protein to a copy of the enzyme. For this, $\mathbf{w}^{u+,b-}$ denotes the modification of $\mathbf{w}$ obtained by adding one to q^u and subtracting one from q^b and $\mathbf{w}^{u-,b+}$ denotes the modification obtained by subtracting one from q^u and adding one to q^b. The fifth case corresponds to a transition due to the completion of enzymatic degradation of a bound copy of a protein. For this, $\mathbf{w}^{b+}$ denotes the modification of $\mathbf{w}$ obtained by adding one to q^b. The seventh case covers a transition due to production of a new copy of the enzyme. For this, $\mathbf{w}^{\ell-}$ denotes the modification of $\mathbf{w}$ obtained by subtracting one from ℓ.

For $i = 1, \ldots, n$, let

$$p_i = \frac{\lambda_i}{\Lambda}.$$

For each $\mathbf{z} = (\mathbf{q}, \ell) \in \mathcal{Z}$, where $\mathbf{q} = (q_1^u, q_1^b, \ldots, q_n^u, q_n^b)$, let $\mathbf{w} = (q^u, q^b, \ell)$ where $q^u = \sum_{i=1}^n q_i^u$, $q^b = \sum_{i=1}^n q_i^b$, and let

$$\chi_{\mathbf{w}}(\mathbf{q}) = \frac{q^u!}{q_1^u! \cdots q_n^u!} \frac{q^b!}{q_1^b! \cdots q_n^b!} \prod_{i=1}^n p_i^{q_i^u + q_i^b}.$$

Theorem 8.1. *Assume that π is a steady-state distribution for $\mathbf{W}$. Then the steady-state distribution for $\mathbf{Z}$ has the following factorized form:*

$$\zeta(\mathbf{z}) = \pi(\mathbf{w}) \chi_{\mathbf{w}}(\mathbf{q}), \quad \mathbf{z} \in \mathcal{Z}. \tag{S20}$$

In other words, in steady-state, conditioned on the value of $\mathbf{W}$, the distribution of the protein types is as if each protein molecule in the system, whether bound or unbound, independently chooses its type, where the probability that it chooses type i is p_i, $i = 1, \ldots, n$.

Proof. Since we assumed that $\mathbf{Z}$ is irreducible and does not explode in finite time, it suffices to show that ζ given by (S20) satisfies the following:

$$\sum_{\tilde{\mathbf{z}} \in \mathcal{Z}} \zeta(\tilde{\mathbf{z}}) \Gamma(\tilde{\mathbf{z}}, \mathbf{z}) = 0 \quad \text{for all } \mathbf{z} \in \mathcal{Z}.$$

We now verify this. In the following, $\mathbf{q}^{i,u-}$ denotes the modification of $\mathbf{q}$ obtained by subtracting one from q_i^u, $\mathbf{q}^{i,u+}$ denotes the modification of $\mathbf{q}$ obtained by adding one to q_i^u, $\mathbf{q}^{i,u+,b-}$ denotes the modification of $\mathbf{q}$ obtained by adding one to q_i^u and subtracting one from q_i^b, $\mathbf{q}^{i,u-,b+}$ denotes the modification of $\mathbf{q}$ obtained by subtracting one from q_i^u and adding one to q_i^b, $\mathbf{q}^{i,b+}$ denotes the modification of $\mathbf{q}$ obtained by adding one to q_i^b.

For any $\mathbf{z} \in \mathcal{Z}$,

$$
\begin{aligned}
&\sum_{\tilde{\mathbf{z}} \in \mathcal{Z}} \zeta(\tilde{\mathbf{z}}) \Gamma(\tilde{\mathbf{z}}, \mathbf{z}) \\
&= \sum_{i=1}^{n} \pi(\mathbf{w}^{u-}) \chi_{\mathbf{w}^{u-}}(\mathbf{q}^{i,u-}) 1_{\{q_i^u > 0\}} \lambda_i + \sum_{i=1}^{n} \pi(\mathbf{w}^{u+}) \chi_{\mathbf{w}^{u+}}(\mathbf{q}^{i,u+}) \gamma(q_i^u + 1) \\
&\quad + \sum_{i=1}^{n} \pi(\mathbf{w}^{u+,b-}) \chi_{\mathbf{w}^{u+,b-}}(\mathbf{q}^{i,u+,b-}) \eta^+(\ell - q^b + 1)(q_i^u + 1) 1_{\{q_i^b > 0\}} \\
&\quad + \sum_{i=1}^{n} \pi(\mathbf{w}^{u-,b+}) \chi_{\mathbf{w}^{u-,b+}}(\mathbf{q}^{i,u-,b+}) \eta^-(q_i^b + 1) 1_{\{q_i^u > 0\}} \\
&\quad + \sum_{i=1}^{n} \pi(\mathbf{w}^{b+}) \chi_{\mathbf{w}^{b+}}(\mathbf{q}^{i,b+}) \mu(q_i^b + 1) + \sum_{i=1}^{n} \pi(\mathbf{w}^{b+,\ell+}) \chi_{\mathbf{w}^{b+,\ell+}}(\mathbf{q}^{i,b+}) \gamma(q_i^b + 1) \\
&\quad + \pi(\mathbf{w}^{\ell-}) \chi_{\mathbf{w}}(\mathbf{q}) \nu(q^u, q^b, \ell - 1) 1_{\{\ell > 0\}} + \pi(\mathbf{w}^{\ell+}) \chi_{\mathbf{w}}(\mathbf{q}) \gamma(\ell - q^b + 1) \\
&\quad - \pi(\mathbf{w}) \chi_{\mathbf{w}}(\mathbf{q}) (\Lambda + \gamma(q^u + \ell) + \mu q^b + \eta^+ q^u (\ell - q^b) + \eta^- q^b + \nu(q^u, q^b, \ell)) \\
&= \chi_{\mathbf{w}}(\mathbf{q}) \left[\sum_{i=1}^{n} \pi(\mathbf{w}^{u-}) \frac{q_i^u}{q^u p_i} \lambda_i 1_{\{q_i^u > 0\}} + \sum_{i=1}^{n} \pi(\mathbf{w}^{u+}) p_i (q^u + 1) \gamma \right. \\
&\quad + \sum_{i=1}^{n} \pi(\mathbf{w}^{u+,b-}) \frac{(q^u + 1) q_i^b}{q^b} \eta^+(\ell - q^b + 1) 1_{\{q_i^b > 0\}} \\
&\quad + \sum_{i=1}^{n} \pi(\mathbf{w}^{u-,b+}) \frac{(q^b + 1) q_i^u}{q^u} \eta^- 1_{\{q_i^u > 0\}} \\
&\quad + \sum_{i=1}^{n} \pi(\mathbf{w}^{b+}) (q^b + 1) p_i \mu + \sum_{i=1}^{n} \pi(\mathbf{w}^{b+,\ell+}) (q^b + 1) p_i \gamma \\
&\quad + \pi(\mathbf{w}^{\ell-}) \nu(q^u, q^b, \ell - 1) 1_{\{\ell > 0\}} + \pi(\mathbf{w}^{\ell+}) \gamma(\ell - q^b + 1) \\
&\quad \left. - \pi(\mathbf{w}) (\Lambda + \gamma(q^u + \ell) + \mu q^b + \eta^+ q^u (\ell - q^b) + \eta^- q^b + \nu(q^u, q^b, \ell)) \right] \\
&= \chi_{\mathbf{w}}(\mathbf{q}) \left[\pi(\mathbf{w}^{u-}) \Lambda 1_{\{q^u > 0\}} + \pi(\mathbf{w}^{u+}) (q^u + 1) \gamma \right. \\
&\quad + \pi(\mathbf{w}^{u+,b-}) (q^u + 1) \eta^+(\ell - q^b + 1) 1_{\{q^b > 0\}} \\
&\quad + \pi(\mathbf{w}^{u-,b+}) (q^b + 1) \eta^- 1_{\{q^u > 0\}} \\
&\quad + \pi(\mathbf{w}^{b+}) (q^b + 1) \mu + \pi(\mathbf{w}^{b+,\ell+}) (q^b + 1) \gamma \\
&\quad + \pi(\mathbf{w}^{\ell-}) \nu(q^u, q^b, \ell - 1) 1_{\{\ell > 0\}} + \pi(\mathbf{w}^{\ell+}) \gamma(\ell - q^b + 1) \\
&\quad \left. - \pi(\mathbf{w}) (\Lambda + \gamma(q^u + \ell) + \mu q^b + \eta^+ q^u (\ell - q^b) + \eta^- q^b + \nu(q^u, q^b, \ell)) \right] \\
&= \chi_{\mathbf{w}}(\mathbf{q}) \sum_{\tilde{\mathbf{w}} \in \mathcal{W}} \pi(\tilde{\mathbf{w}}) \Delta(\tilde{\mathbf{w}}, \mathbf{w}) = 0,
\end{aligned}
$$

where the last equality holds because π is a steady-state distribution for $\mathbf{W}$. □

Under the assumption of Theorem 8.1, we have the following steady-state moment formulas. Let $Q_i = Q_i^u + Q_i^b$ for $i = 1, \ldots, n$. Then $Q = \sum_{i=1}^{n} Q_i$, the total number of copies of proteins in the system.

Corollary 8.1. *In steady-state, for $i = 1, \ldots, n$,*

$$\overline{Q}_i = p_i \overline{Q}, \tag{S21}$$

$$SCV(Q_i) = SCV(Q) - \frac{1}{\overline{Q}} + \frac{1}{\overline{Q}_i}, \tag{S22}$$

and the correlation between Q_i and Q_j for $j \neq i$ is given by

$$\begin{aligned} r_{ij}(\tau = 0) &= \frac{\overline{Q_i Q_j} - \overline{Q}_i \overline{Q}_j}{\sqrt{Var(Q_i) Var(Q_j)}} \\ &= \frac{F-1}{(F-1+\frac{1}{p_i})^{1/2}(F-1+\frac{1}{p_j})^{1/2}}, \end{aligned} \tag{S23}$$

where $F = Var(Q)/\overline{Q}$ is the steady-state Fano factor for Q.

Proof. From Theorem 8.1, in steady-state, conditioned on $\mathbf{W} = (Q^u, Q^b, L) = (q^u, q^b, \ell)$, we have that $(Q_i^u, i = 1, \ldots, n)$ has a multinomial distribution with parameters $(q^u; p_1, \ldots, p_n)$, independent of $(Q_i^b, i = 1, \ldots, n)$ which has a multinomial distribution with parameters $(q^b; p_1, \ldots, p_n)$, and hence $(Q_i, i = 1, \ldots, n)$ has a multinomial distribution with parameters $(q^u + q^b; p_1, \ldots, p_n)$. The formulas for the moments and correlations then follow from computations using these multinomial distributions. These computations are similar to those performed in [4]. We leave the details to the reader. □

Remarks.

1. Note that in order to compute the steady-state Fano factor for Q, one needs to know the steady-state distribution of the three-dimensional Markov chain $\mathbf{W} = (Q^u, Q^b, L)$. However, the dimension can be reduced from three to two, by assuming irreversible, instant binding ($\eta_- = 0, \eta_+ = +\infty$) and that ν depends only on Q. Then (Q, L) is a two-dimensional Markov chain.

2. The reactions in Eq. 3 of the Main Text are nearly the same as those in Eq. 6 of the Main Text when the enzyme E is replaced by the cofactor C, $\nu = \lambda_C$ and $\gamma_C = \gamma$. The only difference is that $X_i C$ degrades to nothing, whereas $X_i E$ degrades to E. Indeed, with a very slight change to the proof of Theorem 8.1, one can show that the factorization result of Theorem 8 and Corollary 8.1 hold when $\mathbf{Z}$ is the Markov chain associated with Eq. 3 of the Main Text. The only difference in the proof is that the infinitesimal generator for $\mathbf{Z}$ associated with Eq. 3 of the Main Text has $\mathbf{z}^{i,b+,\ell+}$ in place of $\mathbf{z}^{i,b+}$ in the fifth line of the description of Γ, and for the infinitesimal generator of $\mathbf{W}$ associated with Eq. 3, in the fifth line of the description of Δ, $\mathbf{w}^{b+}$ is replaced with $\mathbf{w}^{b+,\ell+}$.

3. The result of Theorem 8.1 can be generalized to time-dependent distributions in a similar manner to that in [5] to yield the following: if $\mathbf{Z}$ is initialized with a distribution of factorized form (i.e., conditioned on $\mathbf{W}$, the types of the proteins are distributed as if each protein molecule in the system chooses its type independently of the other protein molecules and such that it is of type i with probability p_i, $i = 1, \ldots, n$), then the distribution of $\mathbf{Z}$ at time t also is of factorized form.

9 Adaptive parallel queueing network with $\nu = \alpha Q_1^u$

We simulated an adaptive parallel enzymatic network with two species where the production rate of the enzyme was proportional to only the unbound molecules of one species. This network exhibited strong correlations for a wide range of λ values and for a large range of the proportionality constant α (Fig. S7).

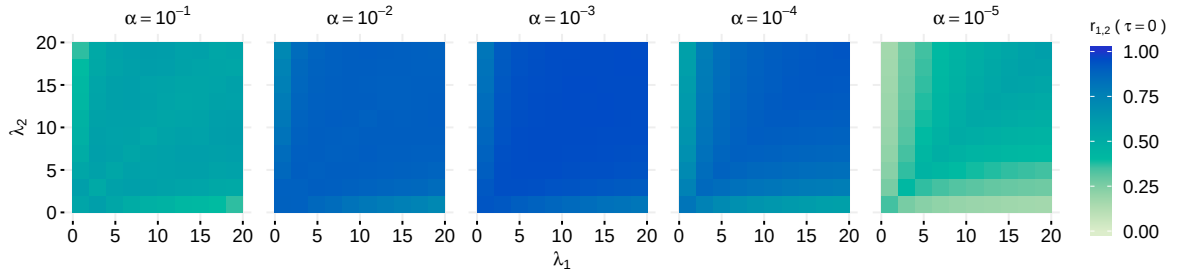

Figure S7: Adaptive parallel network with $\nu = \alpha Q_1^u$ (unbound X_1 only). In the range $10^{-4} < \alpha < 10^{-2}$, adaptation generates strong correlations for nearly all combinations of input rates λ_1 and λ_2. This includes combinations for which λ_1 is an order of magnitude greater or smaller than λ_2. Other parameters were $\mu = 1$, $\eta^+ = 1000$, $\eta^- = 0$, $\gamma = 0.01$

10 Adaptive serial queueing network with $\nu = \alpha Q_1$

We simulated a serial enzymatic adaptive queueing network where production rate of the enzyme was proportional to only one of the proteins. This network also exhibited strong correlations for a wide range of λ values (Fig. S8).

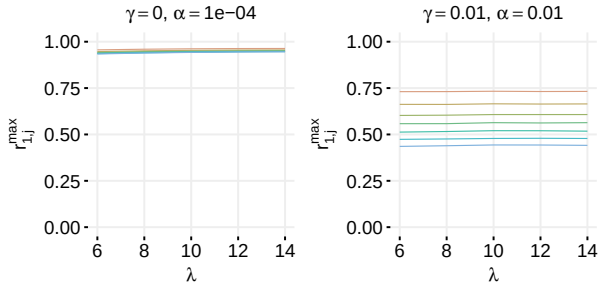

Figure S8: Maximal correlations for an adaptive serial enzymatic network with $\nu = \alpha Q_1$. In this network the synthesis rate of the enzyme is proportional to the total (enzyme-bound and unbound) number of X_1 molecules. Adaptation generates strong correlations for all values of the input rate λ shown without dilution (left) and with dilution (right). Parameters not shown are $\mu = 1$, $\eta^+ = 1000$, $\eta^- = 0$, and the dilution rate for enzymes in both cases is 0.01.

11 Adaptive serial network with $\nu = \nu_0 + \alpha Q_8$

Next we simulated an adaptive serial network with the enzyme synthesized with the rate ν proportional to the amount of total (unbound and enzyme-bound) X_8. In this network, it is possible for enzyme production to permanently cease if enzyme levels and levels of Q_8 are both zero at the same time. To avoid this scenario, we added a small basal level of enzyme production, $\nu_0 = 0.1$, which contributes a mean of $\nu_0/\gamma = 10$ enzymes. The number of enzymes required for adaptation is closer to 80, so this effect is minor. For this network, we again saw adaptation to the critical state. However, the range of usable α values is much narrower (Fig. S9).

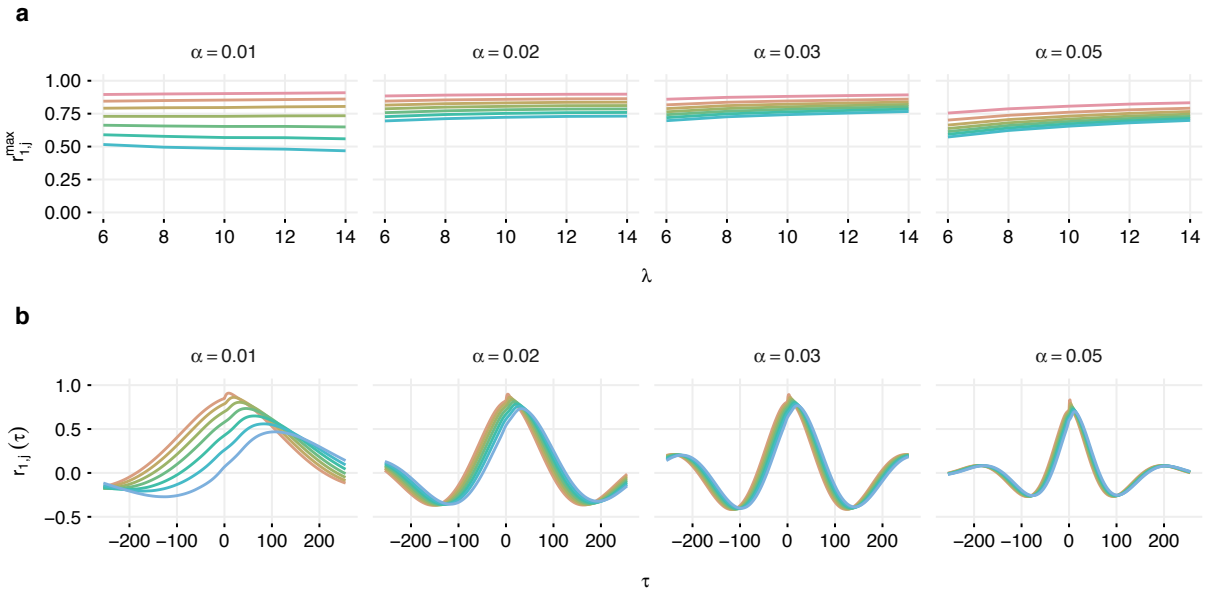

Figure S9: Adaptive serial network with $\nu = \nu_0 + \alpha Q_8$. (a) Maximum correlations between Q_1 and Q_i as a function of λ for different values of the feedback parameter α. For α near 0.02-0.03, correlations between all species are high. (b) Time dependence of correlations for different α with $\lambda = 12$. Negative correlations indicate oscillations of a frequency dependent on α. Other parameter values were $\mu = 1$, $\eta^+ = 1000$, $\eta^- = 0$, $\gamma = 0.01$, $\nu_0 = 0.01$.

12 Serial network adapting to unbound proteins

We also simulated an adaptive serial network with enzyme synthesis rate proportional only to unbound protein (i.e. $\nu = \alpha \sum_i Q_i^u$). Figure S10 illustrates that this network shows very similar behavior to the

network with rate proportional to total protein described in the Main Text.

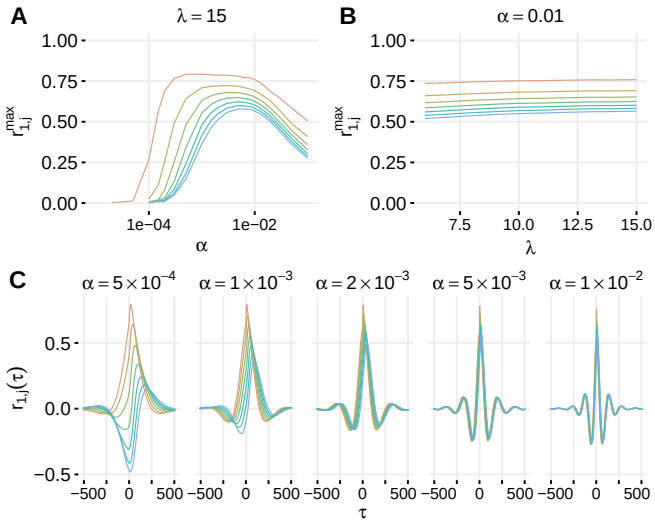

Figure S10: Adaptive serial network with enzyme synthesis proportional to total unbound protein. (A) Maximum correlations between the first species and other species for different values of α when $\lambda = 15$. (B) Maximum correlations between the first species and other species for different values of λ when $\alpha = 0.01$. (C) Time-dependence of correlations for different values of α with $\lambda = 15$. Oscillations increase in frequency as alpha is increased. Parameters for all simulations were $\gamma = 0.01$, $\mu = 1$, $\eta^+ = 1000$, and $\eta^- = 0$.

13 Power spectra of species levels

We computed the power spectral densities of species levels in serial networks. In the constant-enzyme case, there is a large DC component above balance (corresponding to the large nonzero mean of species levels in this regime) and a low DC component below balance. All three cases display similar high frequency power spectra (figure S11).

In order to compare the adaptive case to the non-adaptive case, we modified the non-adaptive network. Enzymes E were produced at a rate λ_E and diluted with other species at the rate γ, giving a mean number of enzymes $\bar{L} = \lambda_E/\gamma$. For $\bar{L} = 80$, this network had a maximum correlation at $\lambda = 11.5$. We then simulated an adaptive network with $\lambda = 11.5$ for various values of the feedback parameter α and computed power spectra (figure S12). We observed apparent amplification of very low frequencies and attenuation of slightly higher frequencies in the adaptive power spectrum, consistent with the oscillations observed in correlations of the adaptive system.

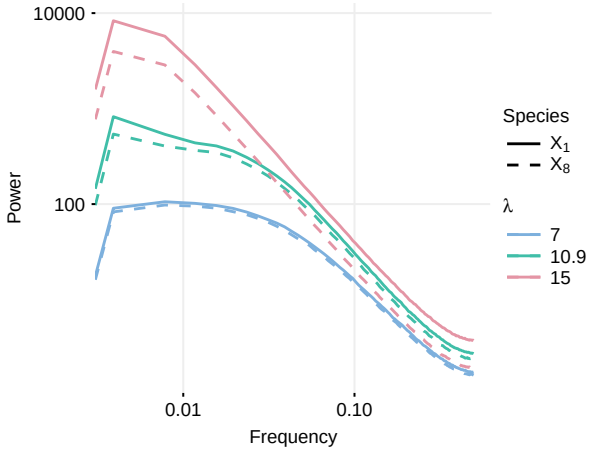

Figure S11: Power spectra in a non-adaptive serial networks below, at, and above balance ($\lambda = 7, 10.9, 15$, respectively). The DC components increase as balance is reached and surpassed, corresponding to the increase in mean species levels. All cases display similar high frequency power spectra. The spectra were estimated using Welch's method. Parameters were $L = 80$, $\gamma = 0.01$, $\mu = 1$, $\eta^+ = 1000$, and $\eta^- = 0$.

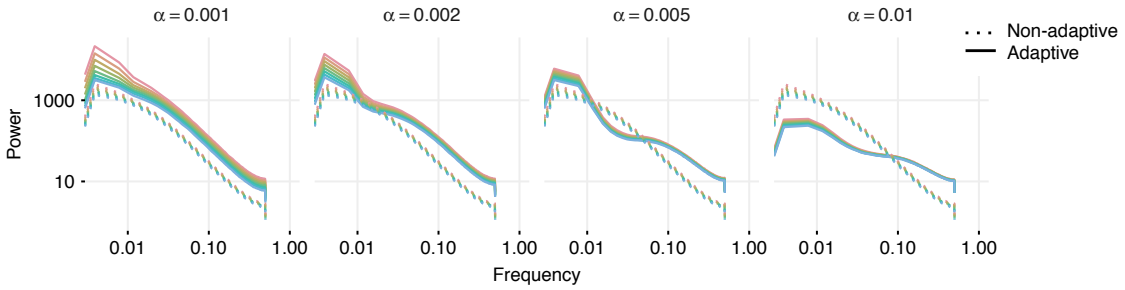

Figure S12: Power spectra in non-adaptive (with stochastic levels of enzyme, see text) and adaptive networks. Adaptive networks for four different values of α are shown; the non-adaptive spectrum is repeated on each plot for reference. The spectra were estimated using Welch's method. Parameters were $\lambda = 11.5$, $\lambda_E = 0.8$, $\gamma = 0.01$, $\mu = 1$, $\eta^+ = 1000$, and $\eta^- = 0$.

References

[1] Gardiner, C. W., 2004. *Handbook of Stochastic Methods.*, 3rd ed. Springer. Berlin.

[2] Gross, D. and C. M. Harris, 1998. *Fundamentals of Queueing Theory.* John Wiley and Sons. New York.

[3] Kelly, F. P., 1979. *Reversibility and Stochastic Networks.* John Wiley and Sons. Chichester.

[4] Mather, W. H., N. A. Cookson, J. Hasty, L. S. Tsimring, and R. J. Williams, 2010. Correlation resonance generated by coupled enzymatic processing, *Biophys. J.* 99: 3172–3181.

[5] Mather, W. H., J. Hasty, L. S. Tsimring, and R. J. Williams, 2011. Factorized time-dependent distributions for certain multiclass queueing networks and an application to enzymatic processing networks, *Queueing Syst.* 69: 311–328.

[6] Norris, J. R., 1997. *Markov Chains.* Cambridge University Press.